PET: The Merging of Biology and Imaging into Molecular Imaging

Michael E. Phelps

Department of Molecular and Medical Pharmacology, Crump Institute for Molecular Imaging and the Department of Energy Laboratory of Structural Biology and Molecular Medicine, School of Medicine, UCLA, Los Angeles, California

PET and SPECT are molecular imaging techniques that use radiolabeled molecules to image molecular interactions of biological processes in vivo. PET imaging technologies have been developed to provide a pathway to the patient from the experimental paradigms of biological and pharmaceutical sciences in genetically engineered and tissue transplanted mouse models of disease. PET provides a novel way for molecular therapies and molecular diagnostics to come together in the discovery of molecules that can be used in low mass amounts to image the function of a target and, by elevating the mass, to pharmacologically modify the function of the target. In both cases, the molecules are the same or analogs of each other. PET can be used to titrate drugs to their sites of action within organ systems in vivo and to assay biological outcomes of the processes being modified in the mouse and the patient. The goal is to provide a novel way to improve the rates of discovery and approval of radiopharmaceuticals and pharmaceuticals. Extending this relationship into clinical practice can improve drug use by providing molecular diagnostics in concert with molecular therapeutics. Diseases are biological processes, and molecular imaging with PET is sensitive and informative to these processes. This sensitivity is exemplified by the detection of disease with PET without evidence of anatomic changes on CT and MRI. These biological changes are seen early in the course of disease, even in asymptomatic stages, as illustrated by the metabolic abnormalities detected with PET and FDG in Huntington's and familial Alzheimer's diseases 7 and 5 y, respectively, before symptoms appear. Differentiation of viable from nonviable tissue is fundamentally a metabolic question, as shown by the use of PET to differentiate patients with coronary artery disease who will benefit from revascularization from those who will not. Although beginning within a specific organ, cancer is a systemic disease the most devastating consequences of which result from metastases. Whole-body PET imaging with FDG enables inspection of glucose metabolism in all organ systems in a single examination to improve the detection and staging of cancer, selection of therapy, and assessment of therapeutic response. In lung and colorectal cancers, melanoma, and lymphoma, PET FDG improves the accuracy of detection and staging from 8% to 43% over conventional work-ups and results in treatment changes in 20%–40% of the patients, depending on the clinical question. Approximately 65% are upstaged because unsuspected metastases are detected, and 35% are downstaged because a structural diagnosis of lesions is changed from malignant to benign. Similar results are now being shown for other cancers. The main difference between CT, sonography, MRI, and PET or SPECT is not technologic but, rather, a difference between detecting and characterizing a disease by its anatomic features as opposed to its biology. The importance and success of developing new molecular imaging probes is increasing as PET becomes integral to the study of the integrative mammalian biology of disease and as molecular therapies targeting the biological processes of disease are developed.

Key Words: PET; molecular imaging; cancer; neurological disease; cardiovascular disease; imaging gene expression

J Nucl Med 2000; 41:661–681

When Watson and Crick elucidated the double-helical structure of DNA in 1958, they made the greatest discovery of this century in the biological sciences. This discovery initiated a time in biology in which biological and physical scientists would strive to unravel the genetic code and its regulated expression, which determines the genotypic basis for the phenotypes of all the cells within the organism. Today, intense exploration is taking place in the biological sciences to determine the patterns of gene expression that encode for normal biological processes, such as replication, migration, signal transduction of cell communication, and the many other functions that cells perform. In addition, belief is growing that most diseases result from altered patterns of gene expression that transition cells to the phenotypes of disease. These alterations in gene expression can result from interactions with the environment, hereditary defects, developmental errors, and aging. As a result, biology is coming together with medicine to design ways to identify these fundamental molecular errors of disease and develop molecular corrections for them. The general name given to this emerging field is molecular medicine.

As biology and medicine come together, it is important that imaging also merge with biology to form the technologies referred to as biological or molecular imaging. This merging is occurring at all levels, from imaging of molecules themselves to imaging of viruses, bacteria, cells, organ systems, and whole organisms. The organisms range from the most simple systems to humans, but in each case,

Received Sep. 30, 1999; revision accepted Dec. 7, 1999.

For correspondence or reprints contact: Michael E. Phelps, PhD, Department of Molecular and Medical Pharmacology, School of Medicine, UCLA, Box 951735, Los Angeles, CA 90095-1735.

imaging is becoming a fundamental technology of integrative biology. The objective of integrative biology is to determine the mechanisms of organized system function. This system may be a protein molecule with many effector sites through which its functions can be altered by interaction with other molecules. The system may also be an organ such as the liver or brain, in which a collection of cells functions as an integrated system based on the molecular mechanisms of intra- and intercellular signal transduction. The role of molecular imaging is to provide technologies that can reveal whole systems and also use molecular probes or interactions to examine the molecular mechanisms of integrated systems. Many imaging technologies have been and are being developed to achieve these goals, such as x-ray diffraction, electron microscopy, optic imaging, autoradiography, MRI, MR spectroscopy, PET, and SPECT. Each has unique applications, advantages, and limitations.

This article focuses on PET, but many of the issues also apply to SPECT. In addition, the article focuses on integrative mammalian biology ranging from the mouse to the human, as well as the transformation of in vitro molecular assays to in vivo imaging. For the purposes of the article, the following provides a conceptual framework:

- All organ functions and diseases have a molecular or biological basis.
- PET and SPECT are molecular imaging technologies.
- Molecular imaging probes are being developed so that PET and SPECT can image and measure the most fundamental biological processes—ranging from transcription and translation of DNA to signal transduction of cell communication—and the synthesis and metabolism of substrates that perform cellular functions.
- The most fundamental way to treat a disease is to correct the original molecular errors of the disease.
- An experimental setting is being developed in which study methods, animal models, and scientific questions are of equal interest to both biologists and imaging scientists. This setting is being achieved by translating experimental biology assays into imaging assays and by developing imaging systems that can examine rodents, which are the focus of mammalian biology today.
- Knowledge gained from molecular imaging assays of animal models is being transferred to molecular imaging examinations of patients.
- Molecular diagnostic imaging will benefit from being developed and aligned with the molecular therapeutics of molecular medicine.

This article discusses ways to approach these issues but is not intended to examine them comprehensively.

PRINCIPLES OF PET

PET is an analytical nuclear medicine imaging technology that uses positron-labeled molecules in very low mass amounts to image and measure the function of biological processes with minimal disturbance (Fig. 1) (*1–5*). Measur-

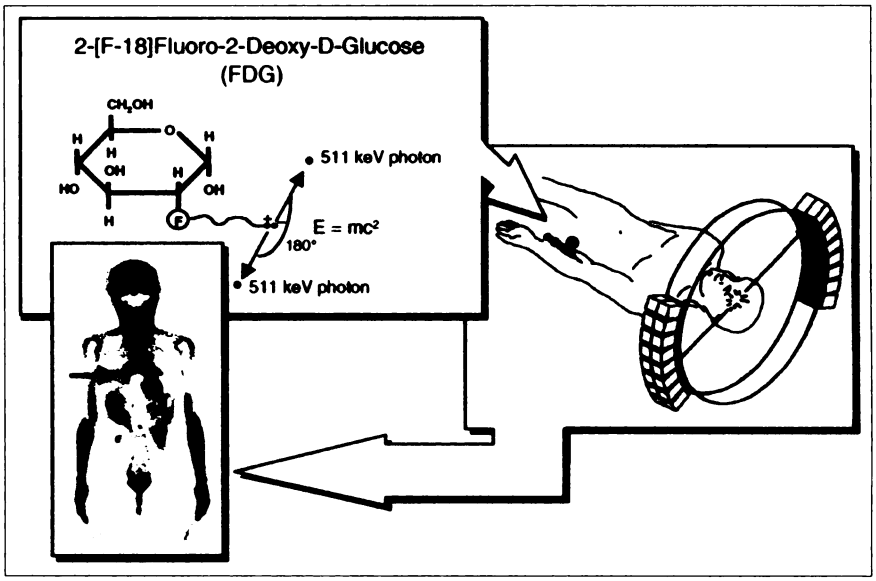

FIGURE 1. Principles of PET. Biologically active molecule is labeled with positron-emitting radioisotope. Example shown is of FDG, which is injected intravenously, distributes through body by way of bloodstream, and enters organs, where it traces transport and phosphorylation of glucose. Two 511-keV photons produced from positron annihilation are detected when these 2 photons strike opposing detectors, providing unique form of electronic collimation. One line of coincidence detection is shown, but in actual tomograph approximately 2–10 million detector pair combinations, or more, can record events simultaneously. Detectors are arranged either in dual-head configuration shown or around entire circumference. Modern dual-head and circumferential PET scanners collect sufficient data to form more than 50 tomographic image planes simultaneously. Tomographic images are collected for selected organ or for entire body. Figure shows single 6-mm-thick coronal plane in woman with bilateral metastasis to lung (arrow) from previous ovarian cancer that was surgically resected. Black is highest metabolic rate in image.

ing without disturbing the biological process is, of course, a fundamental and biologicalally important aspect of the tracer techniques of both PET and SPECT. The assays for PET are developed by first identifying the process to be studied and then synthesizing a positron-labeled molecule through which the assay can be performed. The principle of the assays and the molecular probes originates from basic biological and pharmaceutical science. A biological process is estimated analytically using a compartmental model that describes the process and the way the labeled molecules mimic or trace it. The PET scanner assays the changing tissue concentration of the labeled molecule and its labeled product over time, or their accumulated concentration at a given time, which is determined by the rate of transport and chemical reactions in which the labeled probe participates. Three things allow one to estimate the rate of the biological process studied: first, an input function taken from the plasma to represent the delivery of the labeled probe; second, the PET measure of the tissue concentration of the labeled probe and its labeled reaction products in organs; and third, a compartmental model. Often, the assay models are used to produce sufficient knowledge to allow a simpler, qualitative approach to meet the needs of a clinical service.

Because PET and SPECT scanners cannot directly analyze chemical reaction products in tissue, labeled molecules that mimic a few (1–4) steps of a biological process have to be used so that kinetic analysis can estimate the concentration of reactants and products and the rates of reactions. Many such molecules have been and continue to be developed in biochemistry, pharmacology, and the pharmaceutical industry. Biochemists develop these molecules because of a need to isolate and accurately determine a limited number of chemical steps in a biochemical pathway. Drugs are designed to have limited interactions, because the goal is to modify the function of key steps in a biological process with minimal involvement of other processes.

The molecular imaging of FDG exemplifies isolation and measurement of facilitated transport and hexokinase-mediated phosphorylation of glucose. Sokoloff et al. (*6*) originally developed the method for imaging glycolysis with 2-deoxy-*D*-glucose (2DG) for autoradiography, but Woodward and Hudson (*7*) originally investigated the use of 2DG as a drug to block the accelerated rates of glycolysis in neoplasms by building mass amounts of 2DG-6-PO_4, which inhibits phosphorylation of glucose (*6,7*). Although effective at blocking glycolysis of neoplasms, 2DG in pharmacologic doses was unsuccessful as a drug, because it blocked glucose metabolism in the brain, an organ that cannot switch to alternative substrates, at least in adults. FDG was first synthesized by Ido et al. (*8*), and a compartmental model was developed for quantitative PET studies (*9–11*). FDG has become the most commonly used molecular imaging probe for PET studies of cancer and for the study of normal functions and diseases of the brain and heart. Clinical studies with FDG are qualitative and based on quantitative findings. Thus, the successful imaging probe of 2DG for autoradiography and PET originated from chemical, biochemical, and pharmaceutical investigations.

PET IMAGING IS SENSITIVE TO BIOLOGICAL DISEASE PROCESSES

Because disease is a biological process, molecular imaging should provide a sensitive way to identify and characterize the nature of disease early. A requirement, of course, is use of the labeled molecule specific to the disease of interest.

In the brain, glucose metabolism provides approximately 95% of the adenosine triphosphate (ATP) required for brain function (*12*). FDG is a good probe for general molecular imaging to assess the ATP-dependent function of the brain. The following examples are illustrative.

Dementia

Early clinical diagnosis of the organic dementias remains difficult, as does differentiating specific dementias from each other and from benign reductions in short-term memory and cognitive function in the elderly. More than 4 million Americans now have Alzheimer's disease, with health care expenditures estimated at $50–$70 billion per year (*13,14*). As the baby boomers age, the number of individuals developing Alzheimer's disease will rise sharply, as will the attending costs. Although the molecular errors that cause Alzheimer's disease remain unknown, effective treatments such as the cholinesterase inhibitors, which act as support therapies much like L-dopa for Parkinson's disease, have now been developed. These therapies are most effective when applied early in the disease course, the time at which clinical diagnosis is most difficult. It is estimated that if treatments could reduce the behavioral deficits of Alzheimer's disease, such that patients could lead productive lives and stay out of nursing homes for 5 y, expenditures associated with Alzheimer's would be cut in half.

PET provides an early (Fig. 2), differential (Fig. 3) diagnosis of Alzheimer's disease. These findings have been extensively reviewed in recent years (*15–18*). In longitudinal studies (*19*), PET detected Alzheimer's disease with an accuracy greater than 90% 2.5 y earlier than clinical diagnostic methods using sophisticated university-based evaluations involving blood tests, repetitious neuropsychologic, electroencephalographic, and structural imaging studies. Because many of these comprehensive examinations are usually not performed by general physicians, who see most dementia patients early in the course of their disease, access to an accurate diagnosis through PET is even more beneficial.

PET is also important in the development and assessment of therapies for dementia. One aspect of the contribution of PET is accurate diagnosis at early, more treatable stages of disease, differentiation of Alzheimer's disease from other dementias and normal aging, biological staging as the disease progresses, and biological response to therapy. In addition, the drug itself can be labeled and titrated with PET to the site of action in the brain to determine the degree of

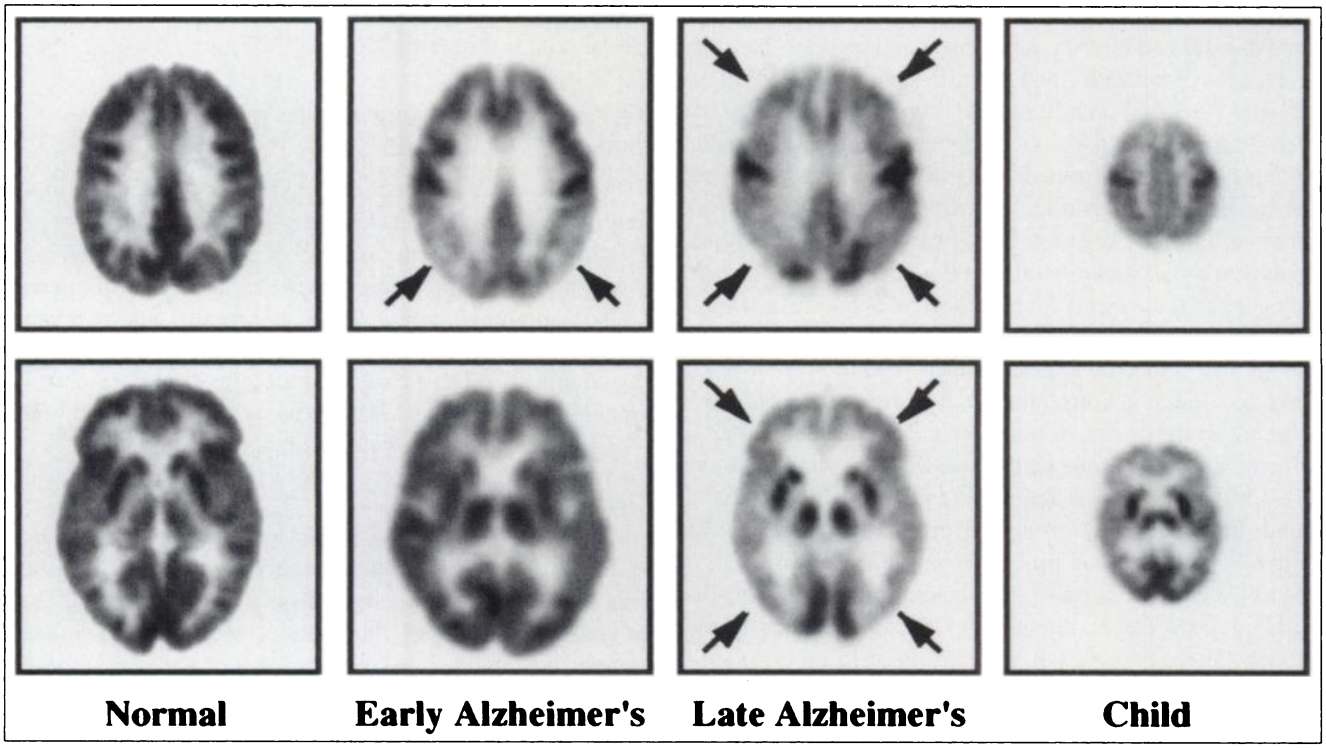

FIGURE 2. PET study of glucose metabolism in Alzheimer's disease. Images were obtained early, at stage of questionable Alzheimer's disease, and illustrate characteristic metabolic deficits in parietal (arrows) and temporal cortices. Over time, metabolic deficit spreads throughout cortex (arrows), sparing subcortical structures and primary sensory areas such as visual and motor cortices. At late stage of disease, metabolic function of brain is similar to that of newborn shown at far right and corresponds to similar behavior and functional capacity. MRI study of patient with early stage of disease showed normal findings. Patient with late stage had some nonspecific atrophy.

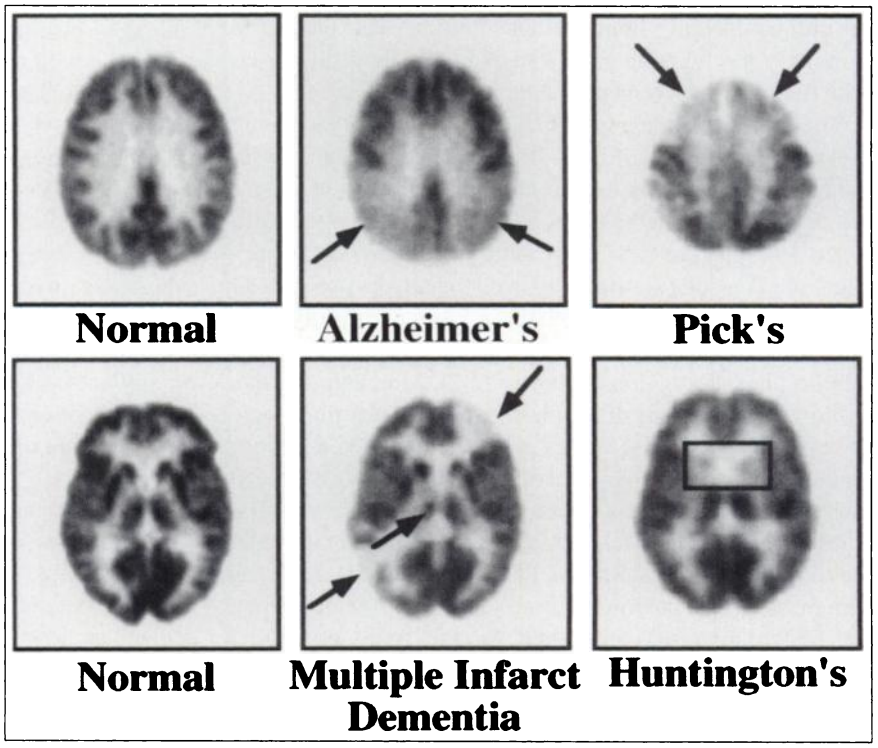

FIGURE 3. PET study of glucose metabolism for differential diagnosis of dementias. Characteristic metabolic deficit in parietal cortex (arrows) in Alzheimer's disease is shown in comparison with frontal metabolic deficit (arrows) in Pick's disease, subcortical metabolic deficits of caudate and putamen (rectangle) in Huntington's disease, and distribution of metabolic deficits (arrows) in multiple-infarct dementia (MID). All patients had normal MRI or CT findings, with exception of MID. Although patient with MID was properly diagnosed by MRI, at autopsy about half of MID patients are found to have Alzheimer's disease with incidental infarcts and to have been misdiagnosed by structural imaging.

occupancy on the target required for effectiveness. This consideration is particularly important, because the administered drug dose and plasma concentration often poorly predict the dose at the site of action within the target tissue. These predictors are inaccurate because of variations caused by systemic factors that alter the amount of intact drug reaching the target and the amount in the tissue that actually interacts with the target molecules.

Detection of Silent, Asymptomatic Disease

Many diseases exist in the body in a silent, asymptomatic phase for a considerable time. Biochemical and transport reserves, as well as redundancies and compensatory responses within the biological processes of organ systems, can prevent the errors of disease from altering the function of an organ system, up to a certain limit. For example, clinical symptoms of Parkinson's disease are not manifested until the substantia nigra loses about 70% of its dopamine neurons. Numerous cancers have been projected to exist years before symptoms result. Although symptoms are not expressed, biological alterations of disease are present and can be detected with molecular imaging probes.

The PET studies of 2 hereditary diseases, Huntington's disease and familial Alzheimer's disease, illustrate the detection of silent, asymptomatic disease. Studying asymptomatic children of patients with Huntington's disease, Mazziotta et al. (*20*) identified metabolic deficits in the caudate and putamen in the fraction of patients in whom mendelian genetics predict the disease. Additionally, all patients who became symptomatic had shown preceding metabolic abnormalities on PET. The longitudinal nature of these studies showed that metabolic abnormalities were detectable approximately 7 y before clinical symptoms appeared.

Small et al. (*21*) and Reiman et al. (*22*) compared metabolic findings with PET to the APOE-4 risk factor for Alzheimer's disease in asymptomatic individuals in families with familial Alzheimer's disease. These investigators found that metabolic deficits in the parietal cortex correlated highly with the presence of APOE-4. Estimates from the study of Small et al. indicate that these deficits were identified with PET approximately 5 y before symptoms were expressed.

Metabolic Viability of Cardiac Tissue

Distinguishing irreversibly damaged tissue from viable tissue is a biological issue. Patients with coronary artery disease have benefited from a variety of treatments, including coronary artery bypass surgery, angioplasty, thrombolysis, heart transplantation, and lifestyle and diet modification. Accurate detection of coronary artery disease and characterization of tissue viability allow effective use of therapies. Schelbert (*23*) developed a PET method for determining the viability and, therefore, reversibility of the effects of coronary artery disease by identifying patients who retained glucose metabolism in the affected myocardial areas (Fig. 4). Although used directly in patients, this method was based on the biochemical principle that glucose is a protective substrate for generating ATP in oxygen-limited states to maintain the viability of tissue despite limitation or loss of local cardiac work (*24*).

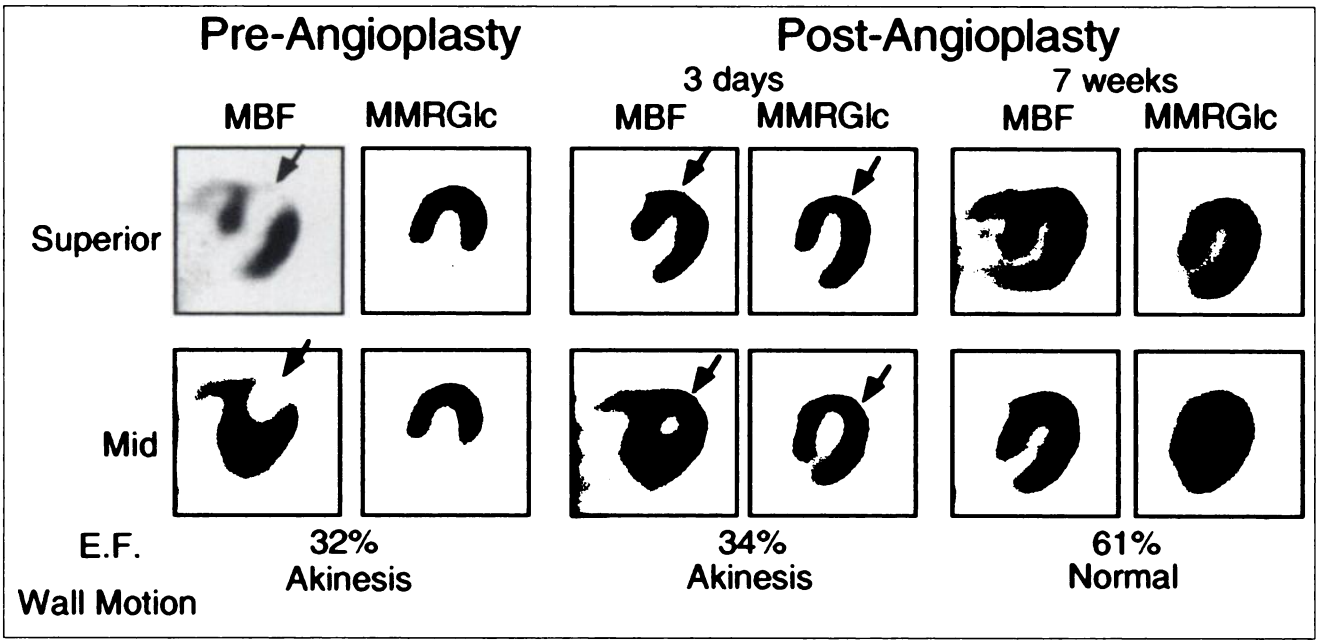

FIGURE 4. PET study of myocardial metabolic rate for glucose (MMRGlc), determined with FDG, and myocardial blood flow (MBF), determined with ^{13}N-NH_3, in patient with coronary artery disease. Preangioplasty study shows blood flow deficit (arrows) caused by occlusion of left anterior descending coronary artery. This segment of tissue, however, retains glucose metabolism, indicating viability and reversibility. Patient has low ejection fraction (E.F.) and akinesis of anterior wall. After angioplasty, myocardial blood flow and glucose metabolism significantly improve by 3 d, yet low E.F. and wall motion abnormalities remain. By 7 wk, myocardial blood flow, glucose metabolism, E.F., and wall motion have returned to normal levels.

Cancer

Cancer biologists have known for decades that neoplastic degeneration is associated with increases in glycolysis because of a progressive loss of the tricarboxylic cycle (TCA) (*25*). Also known is that glucose is used to provide the carbon backbone to meet the high cell replication rates of tumors through activation of the hexose monophosphate shunt (*25*). This knowledge led to the development of 2DG as a potential drug for cancer. A complete loss of the TCA cycle can amplify glucose consumption 19-fold per ATP, because only 2 ATPs are generated when a molecule of glucose is metabolized to lactate, whereas 38 ATPs are generated when a molecule of glucose is completely metabolized to CO_2 and H_2O in the TCA cycle (*26*). Glucose consumption is further amplified by the activation of the hexose monophosphate shunt. These two factors increase glucose consumption as neoplastic degeneration progresses. These high levels of signal in FDG imaging delineate neoplasms from surrounding tissue and detect small lesions. These properties appear to be common for malignancies (Fig. 5).

Cancer is a systemic disease. Although cancer begins within an organ system, the critical feature in treatment and prognosis is metastasis. PET whole-body imaging is an accurate procedure for examining all organ systems for primary and metastatic disease in a single study (*27*). Because whole-body FDG PET detects abnormal tumor metabolism before anatomic change appears and allows differentiation of malignant from benign anatomic abnormalities, 3 benefits are evident:

- Accurate diagnosis of primary and recurrent tumor. Early diagnosis avoids repeated, unsuccessful imaging by less sensitive anatomic techniques and increases the likelihood of tumor eradication before further spread. Greater specificity avoids an erroneous diagnosis of tumor based on benign anatomic changes—particularly important for recurrent tumors, in which new growth must be differentiated from residual edema, necrosis, and scar tissue after previous treatment.
- Accurate determination of tumor extent after diagnosis. Accuracy in staging permits selection of the most appropriate treatment. Identification of metastases that are not seen with conventional imaging (upstaging) avoids the high morbidity and cost of treatments that cannot benefit the patient and permits more effective choices. Likewise, metabolic reclassification of malignant lesions to benign (downstaging) allows patients with false-positive anatomic findings but limited disease to receive potentially curative treatment.
- Prediction and assessment of treatment response. The delay between a metabolic response to therapy and evidence of anatomic changes on conventional imaging may result in multiple cycles of ineffective, morbid, and costly treatment. Similarly, after a therapeutic response is evident, anatomic imaging findings may not clearly indicate when viable tumor has been eradicated and treatment may be ceased, because tumor, edema, and necrosis are not differentiated. In both instances, PET shows a metabolic response in the tumor, permitting timely selection of the best type, dosage, and duration of treatment.

In lung and colorectal cancer, melanoma, and lymphoma, PET has been shown to improve detection and staging by 8%–43% compared with conventional work-ups in head-on comparisons and to change the treatment in 20%–40% of patients (*28–40*). About two-thirds of the treatment changes

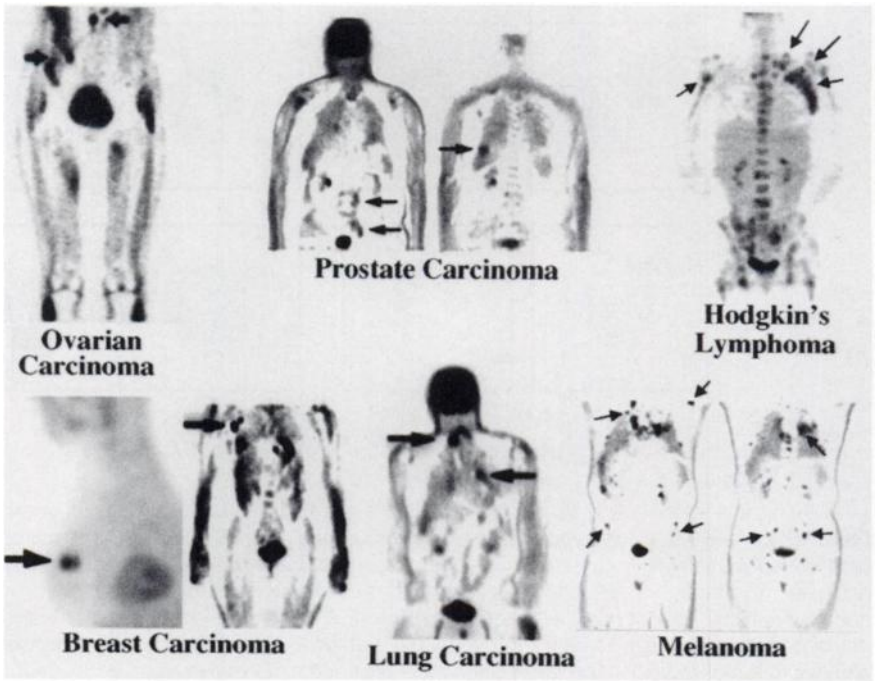

FIGURE 5. Whole-body PET images of glucose metabolism show that increased glycolysis is common in various types of cancer. Arrows point to some lesions.

have been caused by upstaging of disease, whereas one-third have been caused by downstaging. Models have also been developed (*41,42*) as a framework for examining ways to insert PET into the decision-making process and to examine how costs are reduced and care is improved. Because PET alters treatment strategies, such models can assess the benefits and costs as long as good clinical judgment is incorporated in the models and the scientific, medical, and practical factors that affect medical practices are taken into account. For example, these types of analyses often compare PET with a single CT, MRI, or other diagnostic procedure, when in reality, multiple examinations are being performed over time.

Numerous cancer patients today have metastases at the time of initial diagnosis, including many diagnosed with only primary cancer. Detection of disease at late stages, when metastases are present, leads to complicated therapies, limited prognoses, and increased medical care costs. If PET or any other diagnostic test could identify cancer before the gene expression for malignant migration occurs, more patients would be shifted from the group with metastases to the group with only primary cancer. Improved patient outcomes would result, because many primary cancers are curable today, whereas patients with metastases have a poor prognosis. In this way, a diagnostic test could have a profound effect on current treatments.

The rapid growth in cancer biology, genetics, and pharmacology is increasing understanding about the mechanisms of neoplastic degeneration. This understanding will result in treatments directed at molecular characteristics, which are the most critical in therapeutic effectiveness. These advances will also produce opportunities to develop new molecular imaging probes with PET to help improve the diagnosis of cancer, its treatment outcomes, and the overall management of cancer patients. An important goal is to develop probes that identify early transforming cells before gene expression for migration is initiated.

CREATING A NEW EXPERIMENTAL PARADIGM

Biologists, most of whom are not used to working in patient settings, are finding that biology and imaging are merging into laboratory settings in which experimental objectives familiar to them can be pursued. Rodents are the established model for studying modern mammalian biology. Genes are being "knocked in" and "knocked out," and diseased human cells and trophic factors are being transferred to rodents, to study the genotypic basis of normal biological processes and those of disease processes to develop new therapies, including gene therapies. Approximately 2 million genetically engineered mice were produced in the United States in 1999, and this number is expected to triple in the next 3 y from both nonprofit and commercial sources. These activities will continually be refining this approach to modeling human disease.

Biologists are building a line of investigation from genomes, gene expression, protein structures and function, cell and tissue cultures, and simple animal systems to in vitro and in vivo rodent studies. Technology is needed that will allow use of the same types of biological assays in vivo as in vitro. To meet this requirement, imaging scientists are developing in vivo assays that are commonly used by biologists. An example is an assay for imaging and measuring the transcription and translation of gene expression from endogenous and transplanted genes; the transport, metabolism, and synthesis of substrates; and ligand–receptor interactions of cell communication within organ systems. In biology, knowledge grows faster when studies of molecular systems, cell and tissue cultures, and simple animal systems are linked with rodent studies. Molecular imaging is the link between these experimental paradigms and in vivo studies, because the two have molecular assays and biological problems in common.

MICROPET

The design and construction of PET imaging systems for mice and rats are focused on creating an imaging technology for this new experimental paradigm of in vivo integrative, mammalian biology. This exercise is challenging, considering the 2000-fold reduction in size from humans to mice. The goal is to provide a similar in vivo imaging capability in mice, rats, monkeys, and humans so one can transfer knowledge and molecular measurements between species and bring the in-depth understanding gained in genetically engineered mouse models of human disease to the ultimate laboratory setting of the patient.

MicroPET (Concorde Microsystems, Knoxville, TN) technology will be used to illustrate the development of small-animal imaging with PET. The microPET I scanner, developed by Cherry et al. (*43*) and Chatziioannou et al. (*44*), uses a new detector material, lutetium orthosilicate, that has about the same intrinsic efficiency as the commonly used bismuth germanate for detecting the 511-keV photons from positron decay. In addition, lutetium orthosilicate produces about 4–5 times more light and a scintillation decay time that is 8 times faster than bismuth germanate (*45*). Thus, the counting rate capability is increased and random coincident rate is reduced without compromising efficiency. The intrinsic spatial resolution of the microPET I is 1.6 mm full width at half maximum. This device has an image resolution of 1.8 mm (*44*). The use of algebraic reconstruction algorithms that incorporate the detector response function into the reconstruction process improves the resolution to approximately 1.5 mm (*46*). Because the axial field of view of the scanner is 18 mm, whole-body studies in mice and rats are performed by computer-controlled movement of the bed through the scanner gantry, as is done with patients in clinical PET scanners.

Figure 6 compares the quality of images obtained with a clinical PET scanner in patients and a microPET scanner in mice, rats, and monkeys. The images are of local organs and the whole body. Cherry et al. (*47*) designed and are building a microPET II scanner to improve resolution and efficiency

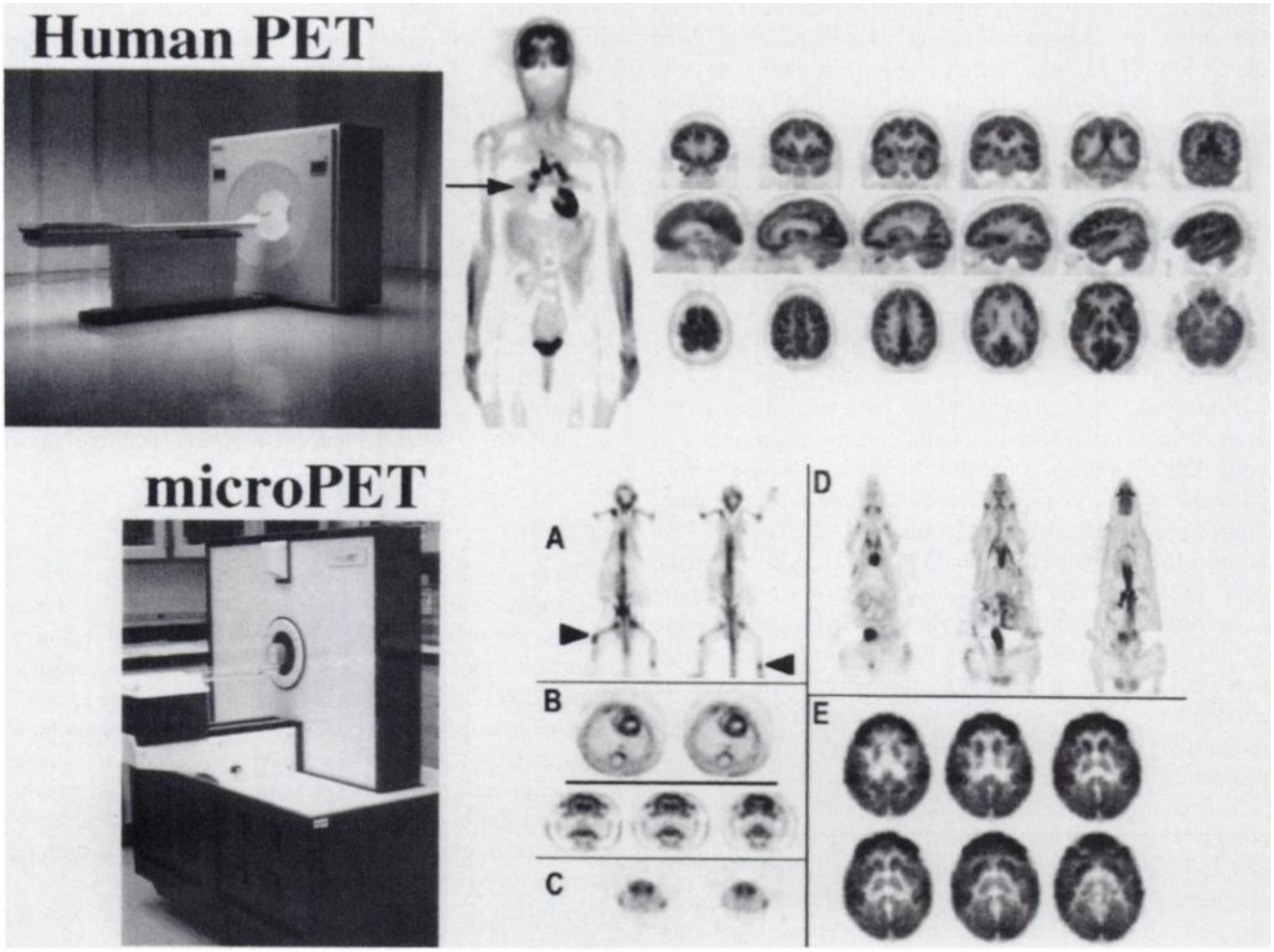

FIGURE 6. Human and microPET I scanners and their corresponding image quality in brain and whole body. Whole-body FDG image of human is 6-mm-thick coronal section with metastases to lung (arrow) from surgically resected ovarian cancer. Human brain images are of healthy volunteer, with top row showing coronal sections, middle row showing sagittal sections, and bottom row showing transverse sections. (A) Two coronal sections of 25-g mouse using ^{18}F-fluoride ion to image skeletal system. Coronal sections are 2 mm thick, and mouse is prostate cancer model with metastases to bone (arrowheads). (B) Cross sections through chest of 250-g rat show, at top, glucose metabolism in left and right ventricle of heart and, at bottom, coronal sections of glucose metabolism in rat brain, indicating that cortex is well separated from striatum. (C) Images of mouse brain with ^{11}C-labeled WIN 35,428, which binds to dopamine reuptake transporter sites and shows clear separation of left and right striatum, which weigh about 15 mg. (D) Coronal whole-body FDG images of glucose metabolism in healthy rat. (E) FDG images of brain of 2-mo-old vervet monkey show good delineation of cortical and subcortical structures. Width of brain is <2 cm. Cortical convolutions are not seen because young monkey brains have few.

and increase the axial field of view, as shown in Table 1. To achieve a volumetric spatial resolution of approximately 1 μL, the system uses lutetium orthosilicate detector elements that are 1 mm high and wide. This system will also use an iterative reconstruction algorithm that incorporates the detector response function, positron range, and angulation error in the 180° emission of photons in positron annihilation to reduce the resolution loss from these factors.

CORRESPONDING STUDY PARADIGMS IN HUMANS AND ANIMALS

The following studies illustrate use of similar types of study paradigms in humans, monkeys, rats, and mice.

Mapping of Stimulation Responses in the Brain

In vivo brain-mapping studies with tomographic imaging began with PET using FDG (*48,49*) in a way similar to studies performed with autoradiography using [^{14}C]deoxyglucose (*6*). This beginning led to the development of the field of brain mapping with PET using, primarily, ^{15}O-labeled H_2O to rapidly measure blood flow (*50*) and functional MRI to measure oxyhemoglobin changes that occur from changes in blood flow and oxygen extraction (*51*).

Figure 7 illustrates the use of microPET I and FDG to map the response to stroking a rat's whiskers with a rod. The images show the metabolic response in the cortical barrels, which receive somatosensory inputs from the whiskers.

TABLE 1
Design Goals of MicroPET II

Characteristic	Value
Spatial resolution	Volume resolution of 1 μL
Efficiency	8 times microPET I
Image plane field of view	10 cm
Axial field of view	8 cm
Physical dimensions	Height, 60 cm; width, 60 cm; thickness, 16 cm

Images of Minibodies

Labeled antibodies have been used for many years in nuclear medicine. Although some success has been achieved, a common problem with antibodies in both therapeutic applications and diagnostic imaging is their large size, which limits diffusion through membranes and makes them attractive targets for degradation by the immune system and enzymes. On the other hand, large reserves of antibodies that target various proteins and other cellular constituents have been produced. These antibodies have been developed by basic biological scientists and are used for in vitro studies that can avoid the complications imposed by their in vivo use. To take advantage of the many well-characterized antibodies, investigators have been developing ways to produce small-molecule versions of antibodies that retain their affinity for a target but are less immunogenic, are not broken down as rapidly by the immune system and enzymes, and have higher membrane permeability. Compounds of this class are often called mimics, because they are smaller versions of the original antibody and can mimic the affinity of the original antibody for the target. They are produced by cloning or synthesizing only the active portion of the antibody. An example of this concept with a genetically engineered minibody against carcinoembryonic antigen (CEA) was developed by Wu et al. (*52*) as an imaging agent labeled with the positron emitter ^{64}Cu, which was supplied by Michael Welch at Washington University. This work used the ^{64}Cu-labeled minibody with microPET in a mouse with a CEA zenograph.

Parkinson's Disease

Parkinson's disease and parkinsonian syndromes are the largest category of movement disorders. An estimated 1 in 200 people more than 50 y old and 1 in 50 more than 60 y old have this disease or these syndromes. Animal models for these disorders often use 1-methyl-4-phenyl-1,2,3,6-tetrahydropyridine (MPTP) or 6-hydroxydopamine lesions of the presynaptic dopaminergic system.

Figure 8 shows multiple imaging studies of a patient with mild Parkinson's disease. The MRI study shows no structural abnormalities in the caudate and putamen, whereas mildly increased glucose metabolism is seen in the putamen because of loss of regulated function in the nigral–striatal pathway. The changes in metabolism are modest, because approximately only 20% of the cells in the caudate and putamen are dopaminergic. More interesting is the severe loss of presynaptic dopamine synthesis and compensatory upregulation of the postsynaptic D_2 receptors in the putamen. Parkinson's disease involves the nigral–putaminal pathway with sparing of the caudate.

An imaging study by Rubins et al. (*53*), shown in Figure 9, had findings similar to those shown in Figure 8 but used the rat model with a presynaptic 6-hydroxydopamine lesion and microPET I. In this case, a unilateral dopamine lesion was used. In rats, the caudate and putamen are not separate but compose a single structure, the striatum. Despite weighing only ~25 mg each, the left and right striatum are well delineated. The presynaptic lesion in the dopamine system and the early postsynaptic compensatory upregulation are well visualized.

In the studies shown in Figures 8 and 9, the brain sizes are approximately 1400 g and 1 g, respectively, yet the integrity of the experiment was reasonably well maintained using a

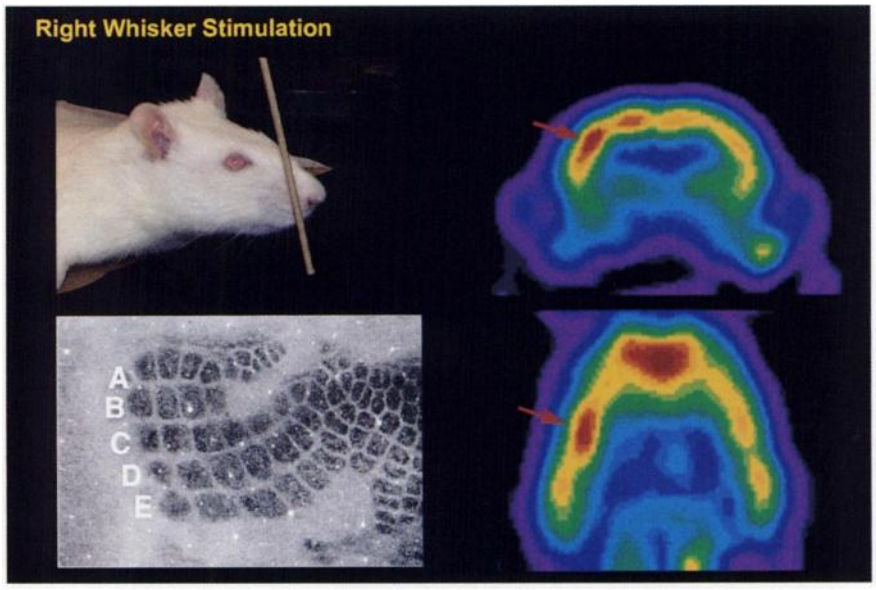

FIGURE 7. MicroPET studies of whisker stimulation in rat. Rod was used to stroke rat's right whiskers after injection of FDG. Each whisker projects to barrel regions (A–E) on cortex, as shown in fluorescent image in bottom left corner. Coronal (top right) and transverse (bottom right) images show glucose metabolic response in brain (arrows).

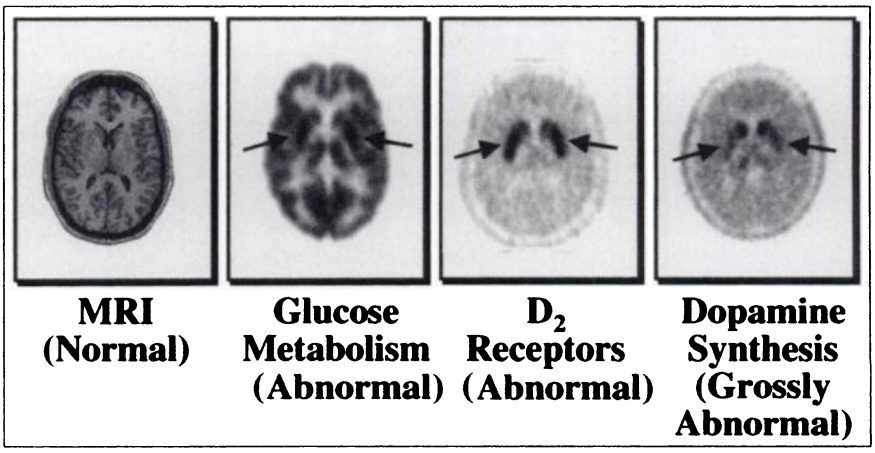

FIGURE 8. MR and PET images of early Parkinson's disease. From left to right, MR image shows normal findings; PET image of glucose metabolism shows hypermetabolic abnormality of putamen (arrows), with approximately 10% increase in metabolism over normal values; [^{18}F]fluoroethylspiperone image shows approximately 15% elevation of D_2 postsynaptic receptors in putamen (arrows); and image of presynaptic dopamine synthesis with [^{18}F]F-dopa shows approximately 70% reduction in dopamine synthesis in putamen (arrows). Black represents highest values in PET images.

PET system designed for humans and another PET system designed for animals.

Figure 10 shows the use of PET to assess a gene therapy approach for restoring dopamine synthesis (K. Bankiewicz, written communication, June 1999). The model was a unilateral MPTP hemiparkinsonism lesion in a monkey. In this case, an adeno-associated virus containing the aromatic amino acid decarboxylase gene was stereotactically injected into striatum lesioned with MPTP to produce the corresponding enzyme for synthesizing dopamine from L-dopa. To determine if the adeno-associated virus had transferred the decarboxylase gene and if the enzyme had been transcribed and translated and was active, dopamine synthesis was imaged with ^{18}F-labeled fluorometatyrosine, which is a substrate for aromatic amino acid decarboxylase. The study indicated that the transfer and production of active enzyme was successful.

IMAGING GENE EXPRESSION IN VIVO

The in vivo imaging of gene expression can be directed either at genes that are externally transferred into cells of organ systems (transgenes) or at endogenous genes, as illustrated in Figure 11. Imaging of transgenes monitors the expression of genes that are transferred into cells to study the normal regulation of gene expression or to produce a therapeutic outcome. Imaging of endogenous gene expression provides the means to examine changes in gene expression during development, aging, and environmental stimulation, as well as those changes that occur when a normal phenotype changes to a phenotype of disease or in response to therapy. Of the 2 approaches to imaging gene expression, imaging endogenous expression is more important, because it is directed at the genotypic basis of the normal phenotypic function of cells and at the alterations of gene expression that can initiate disease. Imaging endogenous gene expression is, however, the more difficult approach.

Imaging Endogenous Gene Expression

Imaging endogenous gene expression can be directed at either transcription of genes into mRNA or translation of mRNA into a protein. Here, the focus is on transcription. The

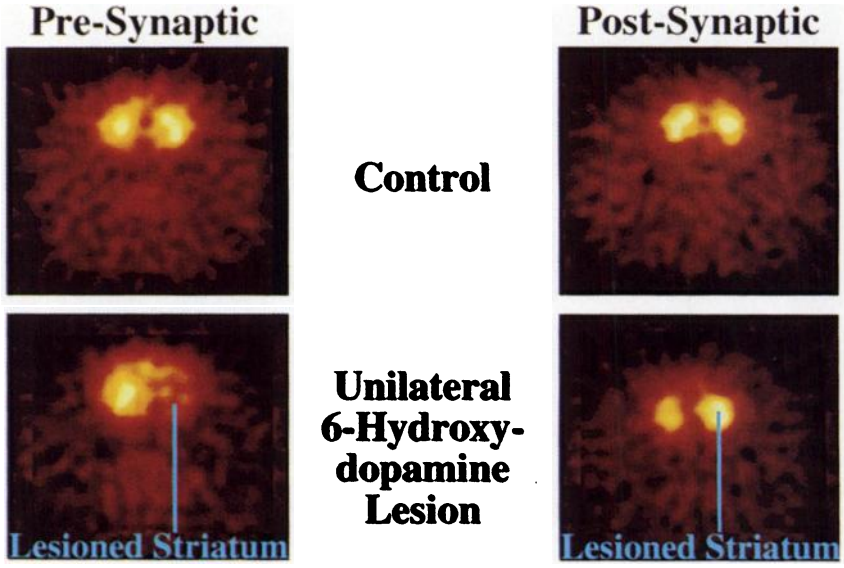

FIGURE 9. MicroPET images of 6-hydroxydopamine unilateral lesion in rat model of hemiparkinsonism. (Top row) Control images of presynaptic system using [^{11}C]WIN 35,425, which binds to dopamine transporters, and corresponding images of postsynaptic D_2 receptors using [^{11}C]raclopride. Left and right striatum of rat are well separated. (Bottom row) Image of lesion (left). Upregulation of D_2 postsynaptic receptors in lesioned striatum is seen in postsynaptic image (right). These rat studies correspond well to patient studies shown in Figure 8. White is highest, and yellow, orange, and red are lower. Courtesy of D. Rubins, W. Melega, S. Cherry, and G. Lacan.

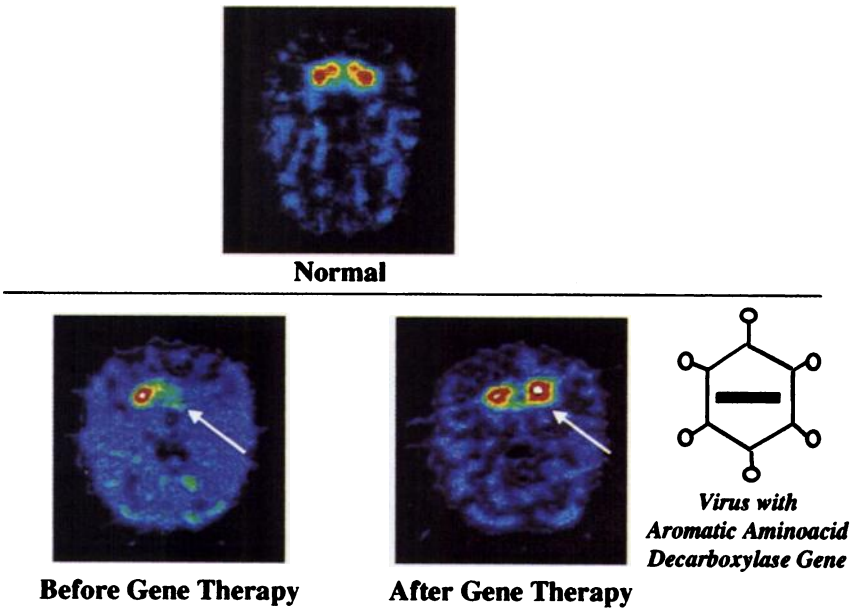

FIGURE 10. Imaging of gene therapy with PET in unilateral MPTP monkey model of hemiparkinsonism. Dopamine synthesis was imaged with [^{18}F]fluorometatyrosine. (Top) Normal dopamine synthesis in single cross section of brain through caudate and putamen. (Bottom left) Unilateral dopamine MPTP-induced deficit (arrow) before gene therapy. (Bottom right) Restoration of dopamine synthesis (arrow) after stereotactic injection of adeno-associated virus containing aromatic amino acid decarboxylase gene to produce corresponding enzyme for dopamine synthesis. Courtesy of K. Bankiewicz, J. Eberling, J. Bringas, P. Pivirotto, J. Harvey-White, J. Cunningham, W. Jaqust, and M. Kohutnicka.

DNA coding process for individual genes is elegantly and systematically defined by the length and ordering of 4 nucleotides: adenine (A), guanine (G), cystine (C), and thymine (T). In the double helix of DNA, the nucleic acids on opposite strands are held in precise registration, with A paired with T and G paired with C. Thus, the 2 strands are complementary. The single strand of mRNA is encoded using A, G, and C, with uracil (U) substituting for the thymine in DNA. The A, G, C, U coding sequence in mRNA is the target for imaging. A modified radiolabeled antisense oligodeoxynucleotide (RASON) coded with the complement of the sequence of a single strand of mRNA is the imaging probe. Applied to PET, this approach converts in situ hybridization to in vivo hybridization. The principles and requirements of this imaging approach were recently reviewed by Gambhir et al. (*54*). Some of the requirements will be briefly summarized to give perspective on the RASON concept. Basic questions include:

- How long a sequence is needed? Mathematical estimates show that only 11–15 bases are required to uniquely select for all the predicted mRNAs expressed from the human genome (*54*). Thus, the RASON can be a fairly small molecule.
- What is the normal range of mRNA concentrations in tissues, and what is the required specific activity of the RASON to image them? Normal mRNA concentrations typically range from 1 to 1000 pmol/L, although in disease conditions such as cancer and viral infections, some mRNAs may be expressed 100–10,000 times higher (*54*). The lower limit of 1 pmol/L will require specific activities of approximately 3.7×10^4 to 3.7×10^5 MBq (10^3–10^4 mCi)/μmol, which is within the range of present positron labeling (*55*).

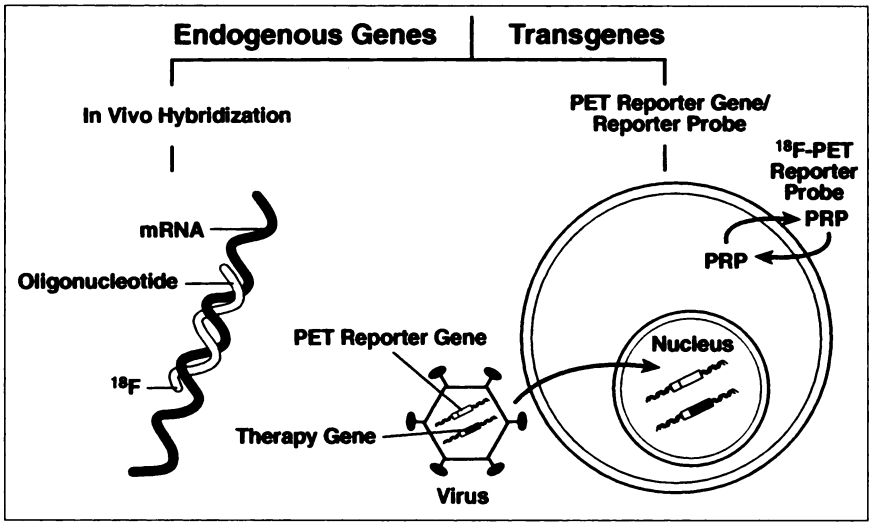

FIGURE 11. Two approaches to imaging gene expression in vivo with PET. At left is approach that images expression of endogenous genes. In situ hybridization is translated to in vivo hybridization using ^{18}F-labeled oligonucleotides that contain complementary sequence of mRNA to be imaged. At right is approach that images transgenes (transplanted genes) administered to subject. PET reporter gene (PRG) and therapy gene with common promoter are administered to subject through vehicle such as virus. Virus transfers PRG and therapy gene to cells of subject. Labeled PET reporter probe (PRP) is then intravenously injected to determine whether gene expression is occurring from PRG.

- Will the RASONs cross cell membranes and have favorable pharmacokinetics? Most oligonucleotides are polyanionic and do not passively diffuse well across membranes. However, processes such as receptor-mediated endocytosis, absorptive endocytosis, and fluid-phase pinocytosis move oligonucleotides across cell membranes, particularly oligonucleotides <30 bases in length (*56,57*). Biodistribution studies of unlabeled phosphorothioate oligodeoxynucleotides have shown them to be stable in vivo, to clear rapidly from plasma, and to have a large volume of distribution, indicating wide access to many tissues in vivo (*58*). Tavitian et al. (*59*) labeled an 18-base phosphorothioate oligodeoxynucleotide with ^{18}F and performed in vivo PET studies in baboons. This RASON was coded for a murine virus. The study was designed to evaluate only the pharmacokinetics of the RASON, not its hybridization to the virus mRNA. The investigators found that labeling with ^{18}F did not alter biodistribution from the native oligodeoxynucleotide. As has been found with an unlabeled oligodeoxynucleotide, this RASON was not significantly degraded, cleared rapidly from plasma, and was widely distributed throughout the tissues of the body, with the exception of the brain (*58*). The specific activity of the RASON used in this study was 7.4×10^4 MBq/μmol (*59*).
- Although a RASON is elegantly coded to specifically bind to the complement code of the target mRNA, to what degree will nonspecific binding occur to and within cells? This critical question remains to be answered.
- How rapidly will the nonspecifically bound RASON clear from tissue to produce an acceptable specific-to-nonspecific ratio? This question is another that is critical and unanswered.

As for all PET assays, the amount of signal produced, the target-to-background ratio, and the specific activity of the probe are critical issues. Imaging expression of endogenous genes can focus on the mRNA or on the protein product of mRNA translation. As the target, mRNA imposes the difficulty of having the lowest concentration, because many proteins are translated from a single mRNA. On the other hand, mRNA as the target has in its favor the elegance of generality; imaging of any gene can be approached by the systematic ordering of a short sequence of only 4 bases in a RASON. For example, 1 can label a single base with ^{18}F, use an automated DNA synthesizer to produce the remainder of the coded sequence, and then connect the ^{18}F-labeled base to form the mRNA-specific RASON, as described by Pan et al. (*55*). The required specific activities can be achieved, but the last 2 questions above remain to be answered.

Targeting the protein product has the advantage of amplifying the target concentration over the concentration of mRNA. If the protein is a receptor, no further amplification occurs, because 1 labeled probe binds to 1 receptor molecule. If the protein is an enzyme, more amplification occurs, because 1 enzyme can produce many labeled metabolic products of the radiolabeled probe. The disadvantage is that a specific labeled ligand or substrate must be developed for each receptor or enzyme product of endogenous gene expression, without a systematic way of constructing probes, as is the case for RASONs.

Imaging Transgene Expression

A transgene is a gene transferred into a subject through a vehicle such as an adenovirus, adeno-associated virus, retrovirus, or liposome or as naked DNA. The imaging objective is to trace the location and temporal changes in expression of the transferred gene. In an example using an adenovirus as the vehicle; the objective is to track a therapy gene. The approach involves converting a technique developed in basic biological sciences—the use of a reporter gene and reporter probe (*60,61*)—into a technique for PET—the use of a PET reporter gene (PRG) and PET reporter probe (PRP) (Fig. 12). The PRG is linked to the therapeutic gene by a common promoter, such as the cytomegalovirus promoter. The promoter initiates transcription of the gene. Thus, when the therapy gene expression is promoted to transcription of mRNA, the same occurs for the PRG. The mRNA of the PRG is then translated to a protein, and this protein is the target of the PRP.

Two PRG and PRP approaches illustrate the concept. In the first, the protein product of the PRG expression is an enzyme, the herpes simplex virus thymidine kinase (HSV-1-TK [by convention, tk and TK refer to the thymidine gene and enzyme, respectively]), and the PRP is 8-[^{18}F]fluoroganciclovir (FGCV), an ^{18}F-labeled analog of ganciclovir, which is a drug used to treat herpes simplex virus (HSV). In the second approach, the PRG protein is a receptor, the dopamine D_2 receptor, and the PRP is [^{18}F]fluoroethylspiperone (FESP), an ^{18}F-labeled D_2 antagonist that was developed by Satyamurthy et al. (*62*) for receptor studies in the brain.

In both approaches, the PRG is incorporated into the genome of an adenovirus, which localizes more than 90% to the liver after intravenous injection in the tail vein of the mouse. The PRP is subsequently injected intravenously to localize and estimate the degree of expression of the PRG.

When HSV-1-tk is used as the PRG, FGCV is injected intravenously, diffuses into cells, and, if no gene expression is present, diffuses out and is cleared to the bladder. If HSV-1-tk gene expression is present, the FGCV is phosphorylated by the HSV-1-TK enzyme to the monophosphate and, then, by cellular kinases to the di- and triphosphates. The phosphorylated FGCV is then trapped in the cell. Thus, the approach is similar to that used with FDG to estimate glycolysis. One molecule of HSV-1-TK can phosphorylate many molecules of FGCV, so that this enzyme-mediated approach has an amplifying effect. Several different substrates for HSV-1-TK have been developed, such as ^{14}C-, ^{131}I-, and ^{124}I-labeled 5-iodo-2′-fluoro-deoxy-1-βD-arabinofuranosyl-5-iodouracil (*63–65*) and FGCV (*54,66–68*) and

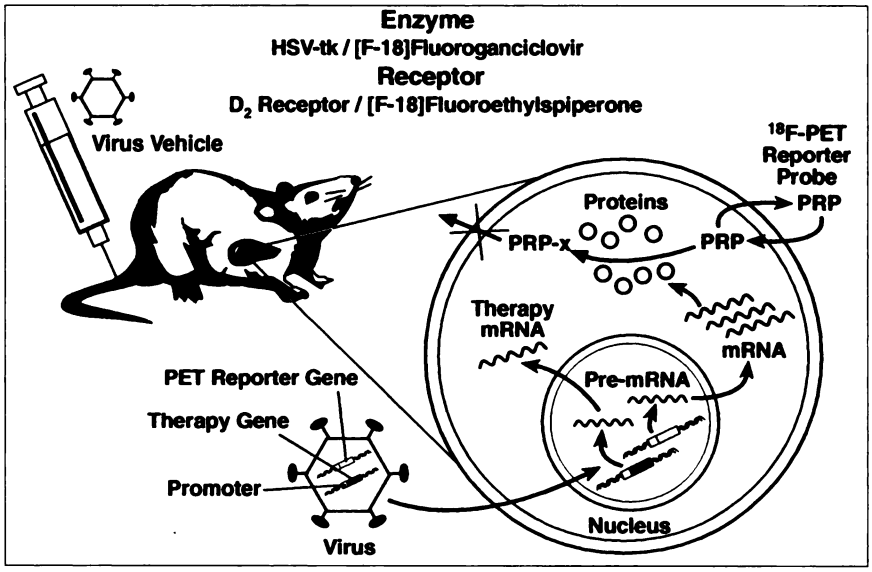

FIGURE 12. PRG–PRP approach using either enzyme or receptor gene as PRG system. In this example, PRG reporter and therapy gene are placed in virus, which is injected into tail vein of mouse. Virus is delivered throughout body by way of bloodstream and localizes in liver. Virus then transfers PRG and therapy gene to cells. Because of common promoter, expression of PRG corresponds to expression of therapy gene. PRG expression proceeds through transcription to mRNA and then translation to protein product. In enzyme example with herpes simplex virus thymidine kinase (HSV-1-tk) gene, protein product is HSV-1-TK enzyme. Animal then receives intravenous injection with the PRP, [^{18}F]fluoroganciclovir, which diffuses into cells. If no gene expression is present, PRP enters and exits cell and is cleared to bladder. If gene expression is present, HSV-1-TK enzyme phosphorylates [^{18}F]fluoroganciclovir, which is retained in cell. In receptor approach, [^{18}F]fluoroethylspiperone is used as PRP to bind to D_2 receptor, which is protein product of PRG.

penciclovir labeled with ^{18}F in the 8 position (*68–71*) or on the side chain (*72*).

In the approach involving the D_2 receptor and FESP (*73*), the protein is a receptor. In this case, gene expression is assayed by ligand–receptor interaction, with the accumulation of ligand depending on the amount of D_2 receptor produced from gene expression of the PRG. The D_2–FESP combination is one in which a single ligand molecule is bound to a single receptor; no amplifying factor is present, as in the case of HSV-1-TK.

Experimental results in mice show that the location and degree of reporter gene expression can be repeatedly imaged in vivo. HSV-1-tk–FGCV examples alternate with D_2–FESP examples, but in each case the same type of study has yielded the same type of result.

Figure 13 is a quantitative comparison between in vivo studies with microPET and autoradiography in the same mouse by MacLaren et al. (*73*). Either a control virus without the D_2 PRG (D_2-) or a virus containing the D_2 receptor gene (D_2+) was injected. Two days later the D_2- animal and the D_2+ animal were injected with FESP to image gene expression with PET. The same animals were then imaged with autoradiography. Correspondence is excellent between the percent injected dose of ^{18}F activity in the liver in comparable longitudinal sections recorded with both imaging techniques. Some activity also appears diffusely throughout the body and in the gastrointestinal tract and bladder, which are the routes of elimination of FESP.

Gambhir et al. (*68*) recently showed that the PRG–probe approach is quantitative and responds linearly using the HSV-1-tk–FGCV system. In these studies, microPET measures of gene expression in mice were directly compared with in vitro measurements of reporter gene expression. The in vitro measurement consisted of assays of mRNA expression by Northern blot analysis and by direct biochemical measures of HSV-1-TK enzyme activity in the liver tissue of mice that underwent in vivo microPET study (*68*). The results show a good linear relationship between the in vivo measure of gene expression with PET and the in vitro measures of HSV-1-tk mRNA and enzyme concentrations (Fig. 14) over the range investigated. Correlation was poor between the amount of virus injected and the amount of expression measured by any of the approaches (*68*). The poor correlation indicates that the external measure of the amount of virus given is not a good measure of the gene therapy dose at the tissue site within the target organ. This finding is common in external drug delivery because of the plethora of systemic effects on the drug and exemplifies another important use of PET—to directly assess drug dosing at the target site within an organ system in vivo. For the D_2–FESP PRG–PRP system a good correlation was found between in vivo PET measured gene expression and in vitro Scatchard analysis of D_2 receptors (*73*).

Figure 15 shows how microPET could be used to repeatedly monitor expression of therapeutic angiogenic genes used for revascularizing ischemic myocardium in rats and to measure the outcome of restoring capillary perfusion. In this example, a common promoter is used to drive the

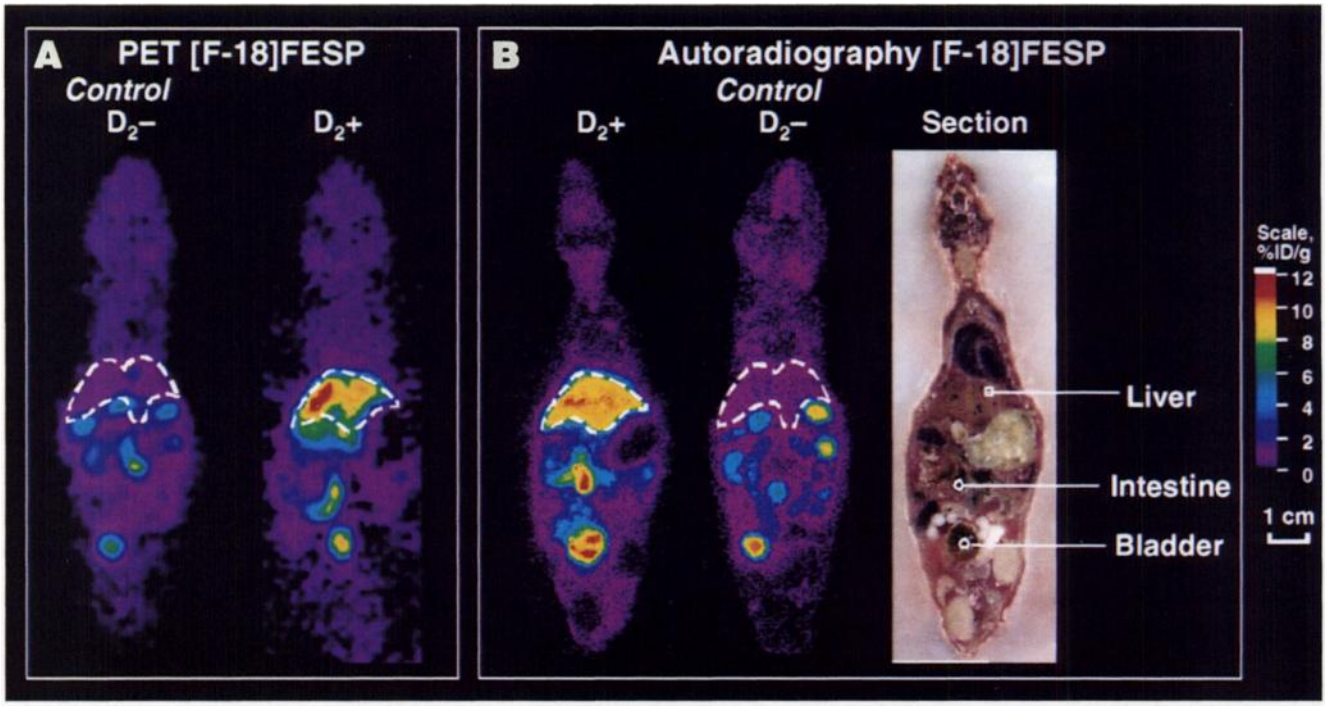

FIGURE 13. MicroPET and autoradiography studies of PRG–PRP imaging of gene expression in same mouse. PRG is D_2 receptor and PRP is FESP. (A) MicroPET image of single coronal section through control mouse negative for D_2 receptor (D_2-). No significant retention of FESP PRP is seen in liver (dashed lines). In animal carrying dopamine receptor reporter gene (D_2+), retention of FESP PRP is seen in liver. Images were taken 60 min after injection of FESP, and studies were performed 2 d after administration of virus. (B) After imaging with microPET, same animals were imaged with autoradiography. Correspondence is good between PET and autoradiography images of gene expression. Photograph of section is shown at far right. Color scales represent quantitative percentage injected dose per gram (%ID/g) of tissue, with red representing highest value.

expression of the PRG and the angiogenic therapy gene, which are connected through an internal ribosome entry site. This genetic construct would be injected directly into the ischemic segment of the heart.

BUILDING A RELATIONSHIP

Although most molecular imaging probes in nuclear medicine originated from molecules developed in industry or the biochemical and pharmaceutical sciences, new relationships are being built more formally. These couple the development and use of diagnostic radiopharmaceuticals and therapeutic pharmaceuticals in a mutually productive manner, combining molecular diagnostics and molecular therapeutics. Academically, the relationships involve nuclear medicine, biology, and pharmacology; commercially, they involve the pharmaceutical, radiopharmaceutical, and imaging industries. The concept begins in the development and use of common molecules or close analogs: molecular imaging probes in low mass amounts to image and measure the function of the target. Then, the mass of the molecule is increased to pharmacologic levels to modify the function of the target. The desired design properties of molecular imaging probes and drugs are similar; although some differences exist, as listed in Table 2.

Just as universities have specific resources, so do the pharmaceutical, radiopharmaceutical, and imaging industries. For example, in several areas today—automated chemical synthesis and screening of molecules with specific

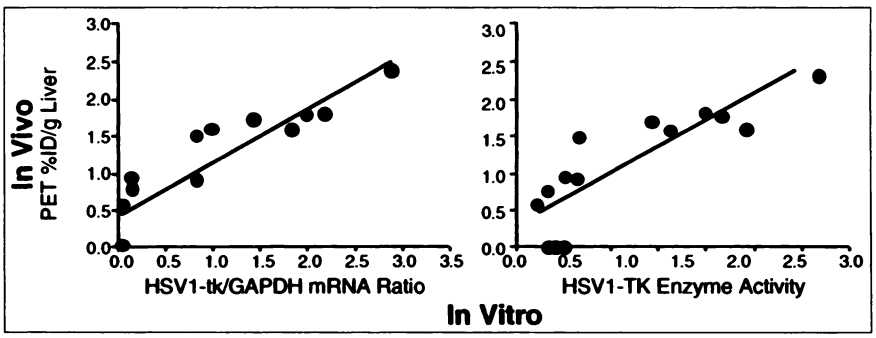

FIGURE 14. Comparison of gene expression measured in vivo with microPET to direct in vitro tissue measures of HSV-1-tk mRNA and HSV-1-TK enzyme activity. Results show excellent correlation between in vivo estimates with PET and direct in vitro measures. GAPDH = reduced glyceraldehyde-phosphate dehydrogenase.

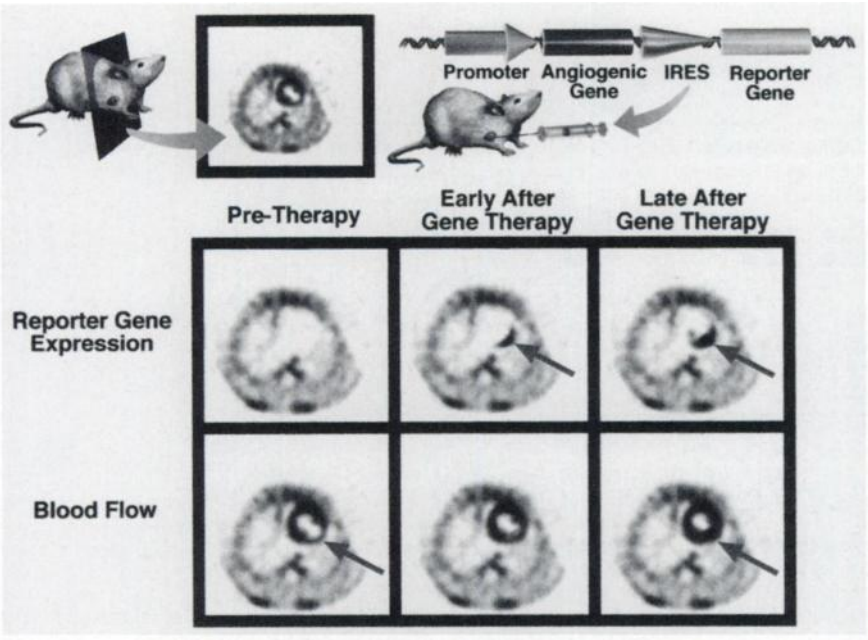

FIGURE 15. Example of use of microPET to monitor location and change in gene expression over time and outcome of gene therapy. Approach uses angiogenic gene for revascularizing ischemic myocardium in which therapeutic and reporter genes are linked to common promoter through internal ribosomal entry site (IRES) and stereotactically injected directly into ischemic myocardium. PET is then used to monitor not only temporal status of gene expression but also restoration of blood flow to ischemic myocardium (arrow). Image of blood flow deficit is from actual microPET I study in rat; remaining images are not actual studies but illustrations of approach.

properties, DNA array technologies, robotics, and information technologies—the capabilities of industry far exceed those of universities. On the other hand, the biology of disease, animal models of disease and patients still remain the domain of schools of medicine and colleges of biological and physical sciences.

Figures 16 and 17 illustrate an approach for combining the resources of universities and the pharmaceutical industry to focus on the mammalian biology of disease and develop diagnostic molecular imaging approaches and therapies. The pharmaceutical industry can rapidly and automatically synthesize thousands of different compounds using such approaches as combinatorial chemistry and can then screen those into smaller groups of, say, tens of different compounds with specific properties (Fig. 16) (*74*). By merging the goals and needs of molecular imaging probes and drugs at the start of this process, molecules can be produced and screened for both purposes. The resultant candidate molecules are the same compound or are analogs of each other.

TABLE 2
Desired Properties of Biological Imaging Probes and Drugs

	Imaging probe	Drug
Small molecule	Yes	Yes
High affinity for target	Yes	Yes
Low affinity for nontargets	Yes	Yes
Require target to background ratio to be >1	Yes	No
Sufficient lipophilicity or carrier system for crossing cell membranes rapidly	Yes	Yes
Clearance from plasma with a half-time of minutes to hours	Yes	No*
Is not rapidly metabolized systematically	Yes	Yes

*Prefer half-times of hours to days

The molecular imaging probes and drugs are then biologically screened and evaluated using an approach, shown in Figure 17, that begins with mouse models of human disease and microPET to evaluate molecular imaging probes and drugs along with traditional pharmacologic, biochemical, and behavioral measures. After studies in a small number of mice, initial studies in patients are performed with the molecular imaging probes and labeled drugs to assess how the findings in mice, to a first approximation, compare with those in patients. When concordance is sufficient, more detailed experiments are performed in an expanded population of mice and then in an expanded population of patients. In this approach, PET characterizes the biology of disease in vivo in mice and patients; titrates the drug to the disease target in tissue for more accurate dosing, using a labeled form of the drug; characterizes the pharmacodynamics and pharmacokinetics of drugs; and assesses, with molecular imaging, the effectiveness of the drug in altering the biological process of the disease.

This approach provides a novel way for the evaluation of both drugs and molecular imaging to be brought together to improve outcomes for both. This paradigm benefits from the rapid evolution of mouse models of disease using transgenes, chimeras, and human tissue transplants and focuses on the biological characteristics of target disease processes in the in vivo setting, which influences these processes in many ways that do not exist in cell and tissue cultures. Performing the same molecular imaging assays in mice and humans provides a scientific bridge between basic and clinical scientists. The assays allow, in patients, much of the biological characterization of disease that is normally limited to the laboratory.

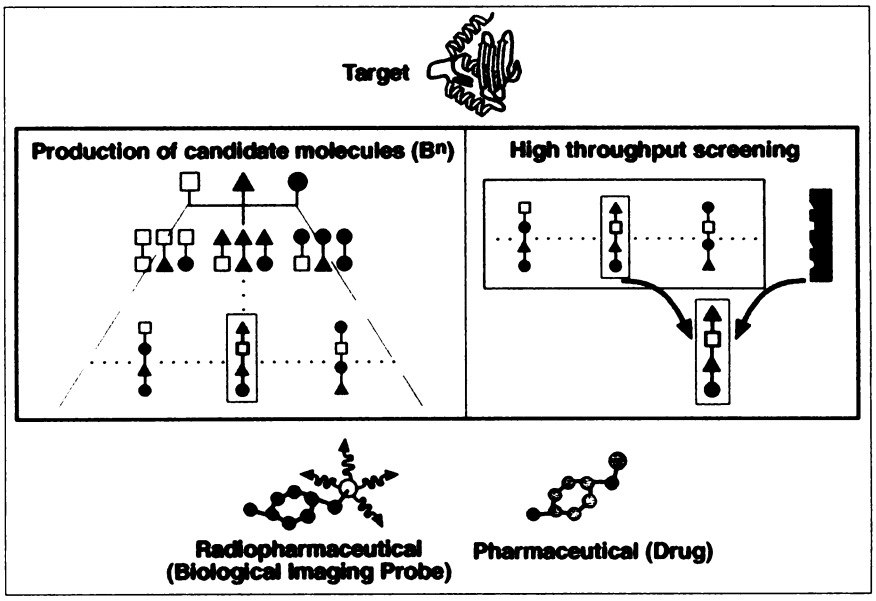

FIGURE 16. Molecular design of pharmaceuticals merged with radiopharmaceuticals using combinatorial chemistry and high-throughput screening. At top is protein target. At left is automated combinatorial chemistry technique for rapidly synthesizing large numbers of candidate molecules. Example begins with 3 compounds that react to produce 9 product compounds. These 9 are then sorted and mixed again to yield 27 new compounds. Final number of compounds is number of starting compounds (B) taken to nth power, where n is number of mix-and-sort steps. For example, taking 3 compounds through 10 steps results in 59,049 compounds. At right is large number of candidate compounds entering high-throughput screening to select those with desired properties. Screen contains molecular and biological properties for selecting appropriate compounds. Smaller number of molecules can then be tested as drugs or labeled and evaluated as molecular imaging probes. Drug and labeled probe can be same molecule or analogs of each other.

ELECTRONIC GENERATORS FOR PET RADIOPHARMACEUTICALS

Many technical innovations have improved PET and made it practical and available to research programs and clinics. Conveniently and cost-effectively labeling compounds with positron radioisotopes has been one of the biggest challenges, in light of the short half-lives of the most common positron-emitting radioisotopes: ^{15}O (2 min), ^{13}N (10 min), ^{11}C (20 min), and ^{18}F (109 min). This challenge required novel approaches to accelerator technology and chemical synthesis.

The largest areas of discovery and innovation in the 20th century have been biology and electronics. Both affect nuclear medicine tremendously. As an illustration of this

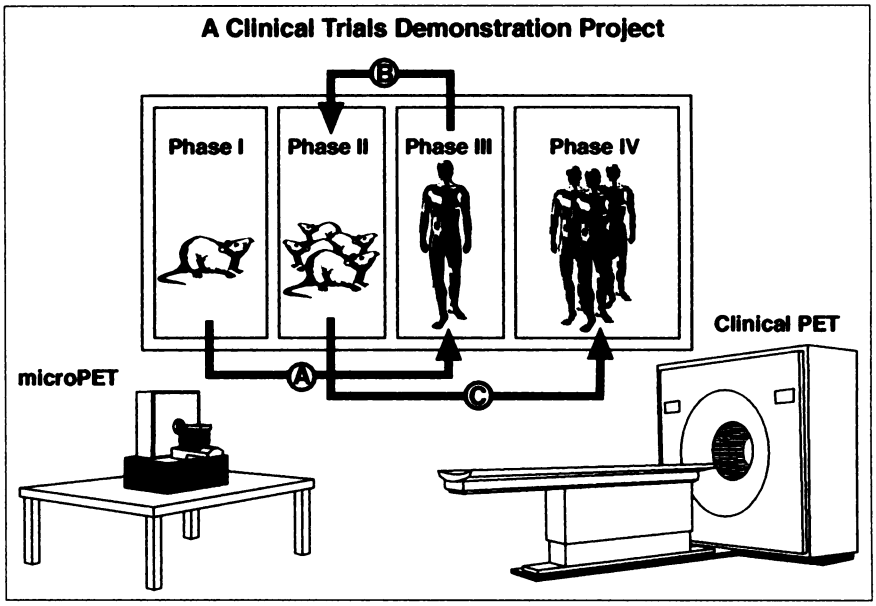

FIGURE 17. Model approach for discovery and evaluation of molecular probes and drugs. Small number of animal models of disease are evaluated with microPET and molecular probes and with direct biological assays and behavioral assessments. If results are positive, small number of studies is performed in patients to assess correspondence between animal model and humans (A). In this case, clinical PET scanner is used to perform same assays in humans as were performed with microPET in animals. If correspondence is reasonable, larger numbers of animals are studied to better define properties of imaging probe or drug (B). Larger number of patient studies are then performed to evaluate approach in humans with clinical PET (C). This approach could be used for evaluating drugs or molecular imaging probes.

effect, consider miniaturized, self-shielded cyclotrons that are integrated with automated chemical synthesizer technology into a system operated by a personal computer (*75*), through which a technologist produces PET radiopharmaceuticals (Fig. 18). The resulting concept is an "electronic generator" for producing PET radiopharmaceuticals. In many ways, these devices are an electronic version of the traditional generators based on ion exchange columns and kits for labeled compound preparations, used in conventional nuclear medicine.

The automated chemical synthesizers of these electronic generators are devices that contain a series of unit chemical processes, such as solvent and reagent addition, column separation, and removal and transfer of solutions. These unit operations can be configured to meet the needs of a particular type of synthesis (*75*). This approach is similar to that used in automated DNA and peptide synthesizers and combinatorial chemistry. The technologic advances in chemical synthesizers for biology and pharmaceutical development are a resource for the continual advancement of automated synthesizers for PET. The commonalities of these technologies for electronic synthesis of compounds illustrates another connection between nuclear medicine, biology, and pharmaceutical sciences.

Electronic generators are operated by a preprogrammed sequence in the personal computer. The program initiates bombardment of a microtarget where the positron radioisotope is produced, automatically transfers the radioisotope to the synthesizer for production of the positron-labeled compound, and automatically transfers the product to a sterile patient vial.

These generators have become the core technology for PET centers and commercial PET radiopharmacies being built worldwide. Like many electronic devices, the generators have high fixed costs and small variable costs. This technology can produce PET radiopharmaceuticals in sufficient volume to control costs and meet the needs of today's medical marketplace.

FROM RESEARCH TO CLINICAL PRACTICE

Figure 19 illustrates the relationship between a PET radiopharmacy, a clinical service, and a molecular imaging laboratory. The PET radiopharmacy provides Food and Drug Administration–approved molecular imaging probes to hospitals for clinical service, labeled compounds to biological or pharmaceutical investigators, and positron radioisotopes to research-based imaging laboratories for the development of imaging probes. The second and third of these functions are similar and commercial delivery of ^{14}C, ^{3}H, ^{32}P, and ^{125}I radioisotopes and labeled compounds to research laboratories. The research component of the radiopharmacy increases the capacity for developing probes and builds relationships with the pharmaceutical industry.

Research imaging laboratories combine cell, tissue, and animal imaging techniques, such as microPET, SPECT, autoradiography, MRI, CT, and optical imaging, with wet laboratories. The locations of this type of imaging laboratory vary. Some are in universities; others are in radiopharmaceutical and pharmaceutical companies. The focus of the programs also varies. Some are directed at the development of new molecular imaging probes and drugs; others, only at drug development. MicroPET and human PET permit movement between animal models and patients with common methods of assessment. Successful outcomes in animals are moved into clinical service, be they radiopharmaceutical or pharmaceutical. Thus, a novel pathway is provided from discovery to clinical use.

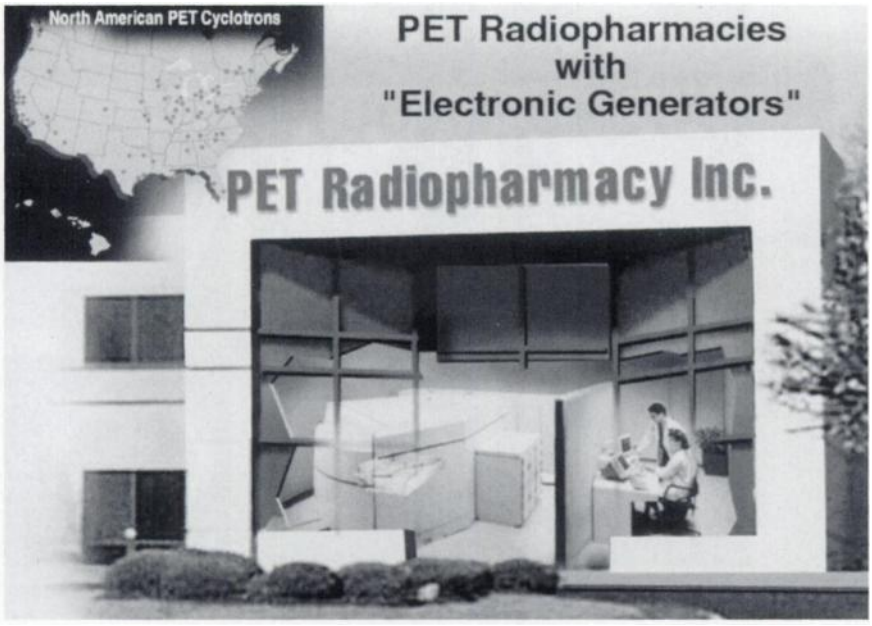

FIGURE 18. Conceptualization of PET radiopharmacies using electronic generators. Electronic generator is miniaturized self-shielded cyclotron integrated with automated chemical synthesizers into single system operated by personal computer. Map shows North American locations of these types of generators for academic programs and radiopharmacies. (PET Radiopharmacy Inc. is generic name.)

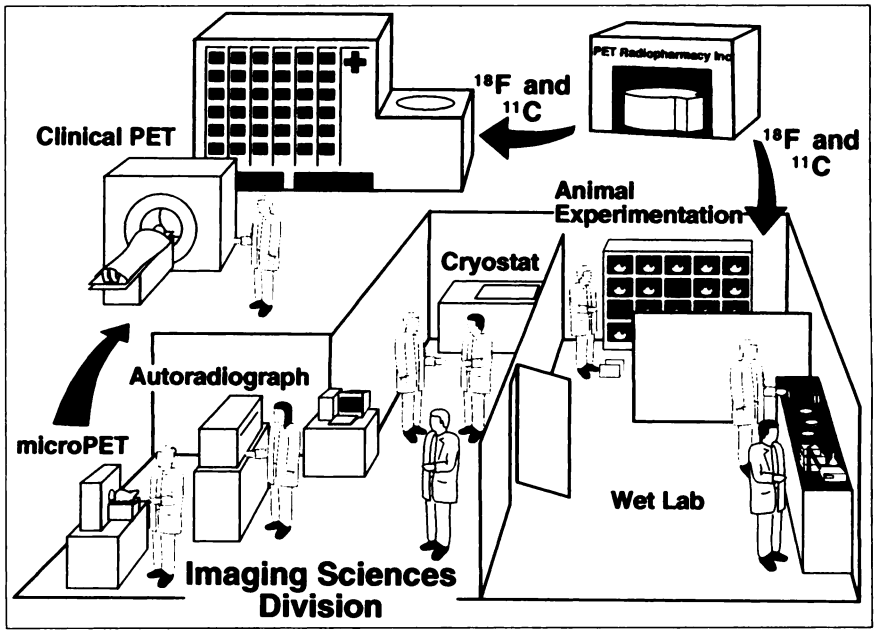

FIGURE 19. Desired relationship between clinical PET services and research and development of PET radiopharmaceuticals. In this model, PET radiopharmacy delivers Food and Drug Administration–approved PET radiopharmaceuticals to clinics. PET radiopharmaceuticals and radioisotopes are delivered to imaging research laboratories. Imaging research laboratories can have small-animal imaging modalities such as PET, MRI, SPECT, CT, autoradiography, and optical imaging systems and wet laboratories for tissue, cell, and chemical analysis. These laboratories are in universities, radiopharmaceutical companies, or pharmaceutical companies and can focus on discovery of molecular imaging probes or pharmaceuticals. Outcomes would be translated into clinical research and, then, clinical practice.

FUSION OF PET AND CT

A new class of imaging technology that fuses 2 technologies is now being developed. These efforts are driven by the desire to merge anatomically and biologicalally based information into a single device, procedure, and image. Although PET and MRI fusion is also being investigated (*76*), the main emphasis is on PET and CT, at both the patient and the small-animal levels.

At the patient level, CT findings are combined with PET to meet several objectives: first, improvement of PET image quality through fast, accurate, and low-noise attenuation correction by CT; second, identification and definition of biological abnormalities by PET, with display of the surrounding anatomy by CT for improved localization; third, planning of surgery, radiation therapy, and biopsy with CT; fourth, better definition of the local separation of diseased tissue, edema, necrosis, and scarring for planning of therapy and evaluation of its outcome, by combining anatomic and

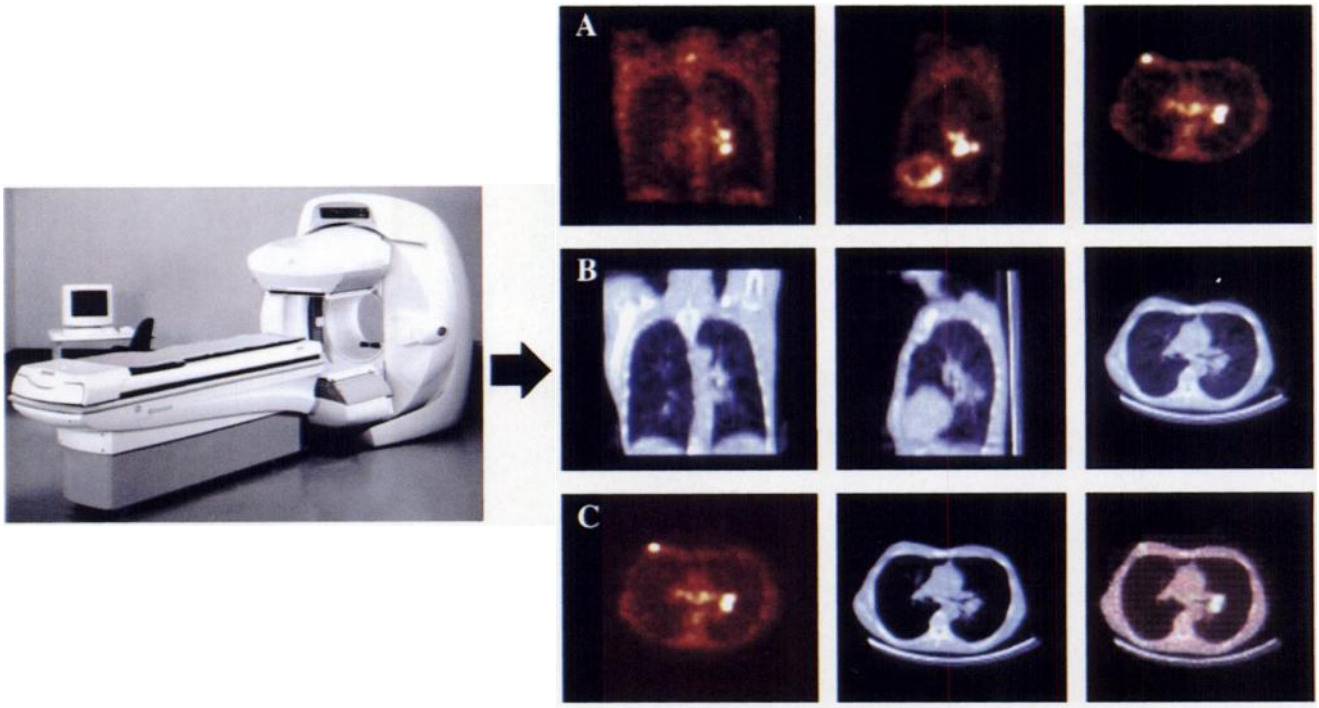

FIGURE 20. System that combines PET and CT. Images are fused to combine anatomic imaging capability of CT with molecular imaging capability of PET. (A) Coronal, sagittal, and transverse FDG PET images of patient with non–small cell lung carcinoma. (B) Corresponding CT images. (C) Fused transverse FDG PET and CT images.

biological information; and fifth, acquisition of CT-based diagnostic information.

Prototype systems have been developed by Beyer et al. (*77*) and CTI/Siemens (Knoxville, TN), using a dedicated PET scanner coupled to a CT scanner, and by Patten et al. (*78*) and General Electric Medical Systems (Milwaukee, WI) (Fig. 20), using a dual-head camera with coincidence detection coupled to a CT scanner. The main philosophic concepts are either to focus on PET and benefit from the first 4 objectives outlined in the preceding paragraph, and to minimize the cost of PET and CT, albeit at a reduction in performance, or to combine a high-end CT scanner and PET scanners to maximize performance to merge state-of-the-art diagnosis from both modalities (the fifth objective) at the expense of a higher cost, while providing the other benefits. Both approaches are being developed. Which solution or whether both will succeed, only time will tell.

The goal in small-animal research is a single device that produces a 3-dimensional volumetric image fusing anatomic and biological information. These devices will provide high throughput, automated analysis of the anatomic localization of biological imaging probes and labeled drugs and would screen for biological responses in transgenics, chimeras, cell transplants, and drug manipulations. The device would also have a stereotactic injector registered by anatomic coordinates for delivering agents and sampling tissue for in vitro analysis. Image quality would also be improved through CT attenuation correction and the use of anatomic information in the PET image reconstruction algorithm. Figure 21 shows an example of such a device.

CONCLUSION

This is a time of explosive growth and change in biology, biological technologies, and medicine. Technology and research in biology are accelerating progress in the emerging field of molecular medicine to identify the molecular errors of disease and to develop molecular therapies.

Nuclear medicine is a molecular imaging discipline, using labeled molecules to show interactions with biological systems of the body much as the pharmaceutical sciences use molecules to produce therapeutic interactions. Disease is a biological process in which molecular errors cause failure of the normal, well-regulated function of cells. Although hereditary errors can be identified by sampling any cell of the body, most diseases occur from alterations within specific organ systems. Even hereditary errors are expressed within specific organ systems. Molecular imaging provides

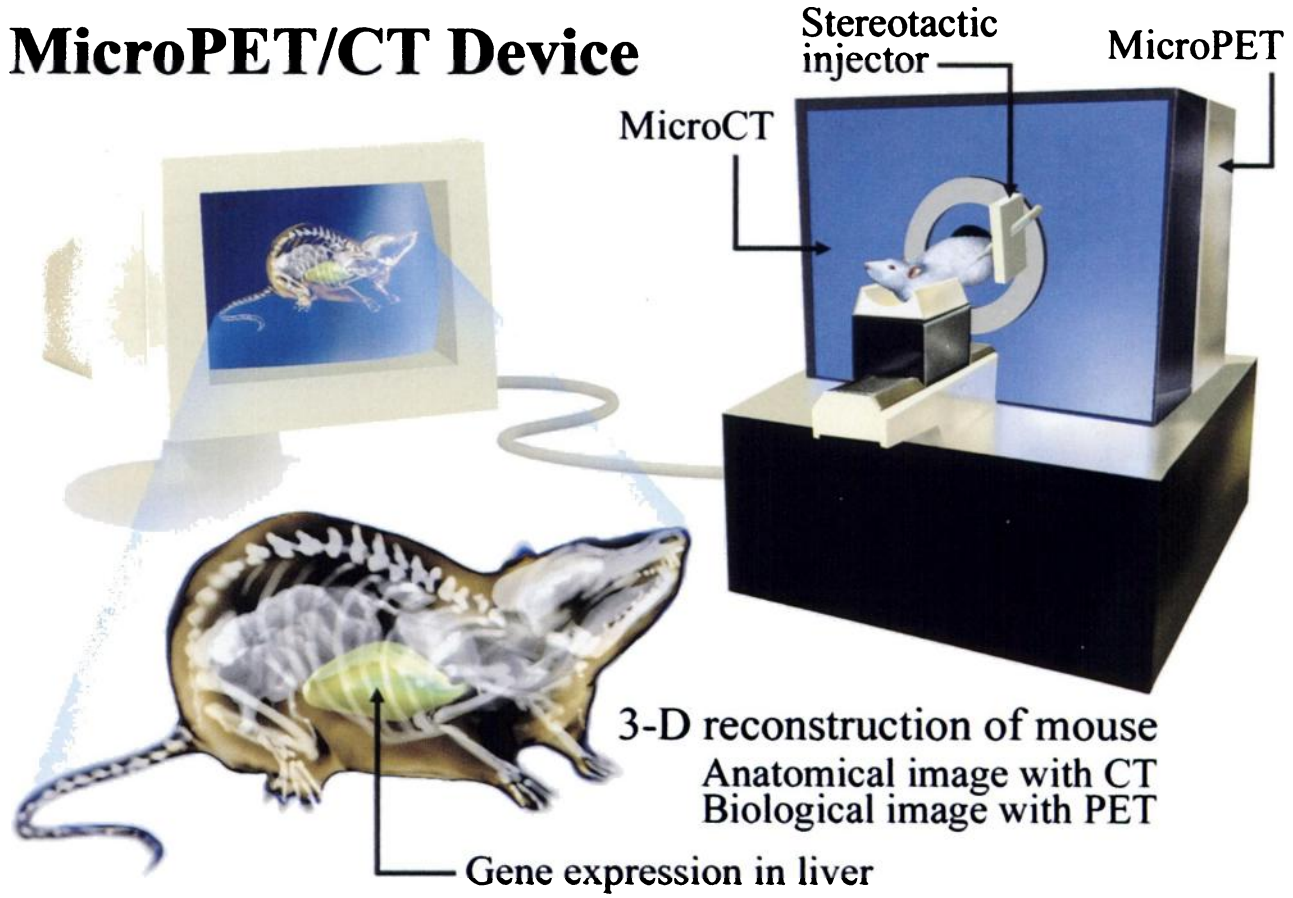

FIGURE 21. Conceptualization of combined small-animal CT and PET scanners under development. Stereotactic injector is attached to device for local organ injections of cells, viruses, and drugs and for tissue sampling for direct biochemical analysis.

the means to examine individual organ systems for these molecular errors of disease.

Nuclear medicine, biology, and the pharmaceutical sciences are joining to build molecules that measure and image biological functions within organ systems and act as drugs to treat disease. Together, these disciplines will accelerate and improve the discovery, approval, and clinical application processes of each. In vivo microimaging laboratories that study the integrative mammalian biology of disease will benefit from biology's use of genetically engineered rodents to study the transformation from normal cells to diseased cells. Biologists will benefit from easier movement from isolated molecular, cellular, and tissue settings to an in vivo setting, where functions are directed and constrained by the requirements of organ systems and whole organisms. Patient care will profit from more direct links between nuclear medicine and pharmaceutical sciences in the areas of molecular diagnostics and molecular therapeutics. The success of this endeavor will require a shared vision between the academic and commercial sectors that encompasses their differing perspectives. The result will be a strong foundation and future for nuclear medicine.

ACKNOWLEDGMENTS

The author thanks Drs. Simon Cherry, Sam Gambhir, Jorge Barrio, Nagichettiar Satyamurthy, Heinz Shelbert, Johannes Czernin, Peter Valk, and Harvey Herschman of UCLA and Dr. Edward Coleman of Duke University for their helpful discussions and comments and Diane Martin and Judy Amos for preparing the manuscript. This work was partially supported by Department of Energy DE-FC03–87ER60615 and the Norton Simon Fund at the University of California, Los Angeles (UCLA), and was taken in part from the 1999 Henry Wagner Lecture given by the author at the annual meeting of the Society of Nuclear Medicine, June 1999.

REFERENCES

1. Phelps M, Hoffman E, Mullani N, Ter-Pogossian M. Application of annihilation coincidence detection to transaxial reconstruction tomography. *J Nucl Med.* 1975;16:210–224.
2. Phelps M, Hoffman E, Mullani N, Higgins C, Ter-Pogossian M. Design considerations for a positron emission transaxial tomograph (PETT III). *IEEE Trans Biomed Eng.* 1976;NS-23:516–522.
3. Hoffman E, Phelps M, Mullani N, Higgins C, Ter-Pogossian M. Design and performance characteristics of a whole body transaxial tomograph. *J Nucl Med.* 1976;493–503.
4. Cho Z, Chan J, Eriksson L. Circular ring transverse axial positron camera for 3-dimensional reconstruction of radionuclide distribution *IEEE Trans Nucl Sci.* 1976;NS-23:613–622.
5. Derenzo S, Budinger T, Cahoon J. High resolution computed tomography of positron emitters. *IEEE Nucl Sci.* 1977;NS-24:544–558.
6. Sokoloff L, Reivich M, Kennedy C, et al. The (^{14}C) deoxyglucose method for the measurement of local glucose utilization: theory, procedure and normal values in the conscious and anesthetized albino rat. *J Neurochem.* 1977;28:897–916.
7. Woodward GE, Hudson MT. The effect of 2-deoxy-D-glucose in glycolysis and respiration of tumor and normal tissues. *Cancer Res.* 1954;14:599–605.
8. Ido T, Wan C-N, Casella JS, et al. Labeled 2-deoxy-D-glucose analogs: ^{18}F labeled 2-deoxy-2-fluoro-D-glucose, 2-deoxy-2-fluoro-D-mannose and ^{14}C-2-deoxy-2-fluoro-D-glucose. *J Labeled Compds Radiopharmacol.* 1978;14:175–183.
9. Phelps ME, Huang SC, Hoffman EJ, Selin C, Sokoloff L, Kuhl DE. Tomographic measurement of local cerebral glucose metabolic rate in humans with (F-18) 2-fluoro-deoxy-D-glucose: validation of method. *Ann Neurol.* 1979;6:371–388.
10. Reivich M, Kuhl D, Wolf A, et al. The (^{18}F)fluorodeoxyglucose method for the measurement of local cerebral glucose utilization in man. *Circ Res.* 1979;44: 117–127.
11. Huang SC, Phelps ME, Hoffman EJ, Sideris K, Selin C, Kuhl DE. Noninvasive determination of local cerebral metabolic rate of glucose in man. *Am J Physiol.* 1980;238:E69–E82.
12. Sokoloff L. Circulation and energy metabolism of the brain. In: Siegel G, Agranoff B, Albers RW, Molinoff P, eds. *Basic Neurochemistry.* 4th ed., New York, NY: Raven; 1989:565–590.
13. Ernst RL, Hay JW. The U.S. economic and social costs of Alzheimer's disease revisited. *Am J Pub Health.* 1994;814:1261–1264.
14. National Institute on Aging. *Progress Report on Alzheimer's Disease.* NIH Publication 96–4137. Bethesda, MD: National Institute on Aging; 1996.
15. Dura R, Grady C, Haxby J, et al. Positron emission tomography in Alzheimer's disease. *Neurology.* 1986;36:879–887.
16. Mazziotta JC, Frackowiak RSJ, Phelps ME. The use of positron emission tomography in the clinical assessment of dementia. *Semin Nucl Med.* 1992;22: 233–246.
17. Herholz K. FDG PET and differential diagnosis of dementia. *Alzheim Dis Assoc Disord.* 1995;9:6–16.
18. Silverman DHS, Small GW, Phelps ME. Clinical value of neuroimaging in the diagnosis of dementia: sensitivity and specificity of regional cerebral metabolic and other parameters for early identification of Alzheimer's disease. *Clin Positron Imaging.* 1999;2:119–130.
19. Silverman DHS, Chang CY, Cummings J, et al. Neuroimaging in evaluation of dementia: regional brain metabolism and long-term clinical outcomes. *Ann Intern Med.* 2000: in press.
20. Mazziotta JC, Phelps ME, Huang SC, et al. Cerebral glucose utilization reductions in clinically asymptomatic subjects at risk for Huntington's disease. *N Engl J Med.* 1987;316:357–362.
21. Small GW, Mazziotta JC, Collins MT, et al. Apolipoprotein E type 4 allele and cerebral glucose metabolism in relatives at risk for familial Alzheimer disease. *JAMA.* 1995;273:942–947.
22. Reiman EM, Caselli RJ, Yun LS, et al. Preclinical evidence of Alzheimer's disease in persons homozygous for the E4 allele for apolipoprotein E. *N Engl J Med.* 1996;334:752–758.
23. Schelbert HR. The usefulness of positron emission tomography. *Curr Probl Cardiol.* 1998;2:69–120.
24. Ausma J, Thonae F, Dispersyn GD, et al. Dedifferentiated cardiomyocytes from chronic hibernating myocardium are ischemia-tolerant. *Mol Cell Biochem.* 1998:186:159–168.
25. Weber G. Enzymology of cancer cells. *N Engl J Med.* 1977;296:541–551.
26. White A, Handler P, Smith E. *Principles of Biochemistry.* 5th ed. New York, NY: McGraw-Hill; 1973:441.
27. Dahlbom M, Hoffman E, Hoh C, et al. Evaluation of a positron emission tomography scanner (PET) for whole body imaging. *J Nucl Med.* 1992;33:1191–1199.
28. Valk PE, Pounds TR, Hopkins DM, et al. Staging non-small-cell lung cancer by whole-body PET imaging. *Ann Thorac Surg.* 1995;60:1573–1582.
29. Changlai SP, Schiepers C, Blatt SA, et al. The impact of whole body FDG PET on staging of lung cancer [abstract]. *J Nucl Med.* 1999;40(suppl):56P.
30. Valk PE, Pounds TR, Tesar RD, Hopkins DM, Haseman MK. Cost-effectiveness of PET in clinical oncology. *Nucl Med Biol.* 1996;23;737–743.
31. Marom EM, McAdams HP, Erasmus JJ, et al. Staging non-small cell lung cancer with whole-body PET. *Radiology.* 1999;212:803–809.
32. Vitola JV, Delbeke D, Sandler MP, et al. Positron emission tomography to stage suspected metastatic colorectal carcinoma to the liver. *Am J Surg.* 1996;171: 21–26.
33. Beets G, Penninckx F, Schiepers C, et al. Clinical value of whole-body positron emission tomography with [^{18}F]fluorodeoxyglucose in recurrent colorectal cancer. *Br J Surg.* 1994:81:1666–1670.
34. Lai DTM, Fulham M, Stephen MS, et al. The role of whole-body positron emission tomography with [^{18}F]fluorodeoxyglucose in identifying operable colorectal cancer metastases to the liver. *Arch Surg.* 1996;131:703–707.
35. Valk PE, Abella-Columna E, Haseman MK, et al. Whole-body PET imaging with F-18-fluorodeoxygluose in management of recurrent colorectal cancer. *Arch Surg.* 1999;134:503–511.
36. Ogunbiyi OA, Flanagan FL, Dehdashti F, et al. Detection of recurrent and metastatic colorectal cancer: comparison of positron emission tomography and computed tomography. *Ann Surg Oncol.* 1997;4:613–620.

37. Damian DL, Fulham MJ, Thompson E, Thompson JF. Positron emission tomography in the detection and management of metastatic melanoma. *Melanoma Res.* 1996;6:325–329.
38. Rinne D, Baum HP, Hor G, Kaufmann. Primary staging and follow-up of high risk melanoma patients with whole-body ^{18}F-fluorodeoxyglucose positron emission tomography. *Cancer.* 1998;82:1664–1671.
39. Stumpe KDM, Urbinell M, Steingert HC, et al. Whole-body positron emission tomography using fluorodeoxyglucose for staging of lymphoma: effectiveness and comparison with computed tomography. *Eur J Nucl Med.* 1998;25:721–728.
40. Moog F, Bangerter M, Diedrichs CG, et al. Extranodal malignant lymphoma: detection with FDG PET versus CT. *Radiology.* 1998;206:475–481.
41. Gambhir SS, Hoh CK, Phelps ME, Madar I, Maddahi J. Decision tree sensitivity analysis for cost-effectiveness of FDG-PET in the staging and management of non-small-cell lung carcinoma. *J Nucl Med.* 1996;37:1428–1436.
42. Gambhir SS, Shepherd JE, Shah BD, et al. An analytical decision model for the cost-effective management of solitary pulmonary nodules. *J Clin Oncol.* 1998;16: 2113–2125.
43. Cherry SR, Shao Y, Silverman RW, et al. MicroPET: a high resolution PET scanner for imaging small animals. *IEEE Trans Nucl Sci.* 1997;44:1109–1113.
44. Chatziioannou AF, Cherry SR, Shao Y, et al. Performance evaluation of microPET: a high resolution lutetium oxyorthosilicate PET scanner for animal imaging. *J Nucl Med.* 1999;40:1164–1175.
45. Casey ME, Eriksson L, Schmand M, et al. Investigation of LSO crystals for high spatial resolution positron emission tomography. *IEEE Trans Nucl Sci.* 1997;44: 1109–1113.
46. Qi J, Leahy RM, Cherry SR, Chatziioannou A, Farquhar TH. High resolution 3D Bayesian image reconstruction using the microPET small animal scanner. *Phys Med Biol.* 1998;43:1001–1013.
47. Cherry SR, Shao Y, Slates RB, Wilcut E, Chatziioannou AF, Dahlbom M. MicroPET II: design of a 1 mm resolution PET scanner for small animal imaging [abstract]. *J Nucl Med.* 1999;40(suppl):75P.
48. Phelps ME, Kuhl DE, Mazziotta JC. Metabolic mapping of the brain's response to visual stimulation: studies in humans. *Science.* 1981;211:1445–1448.
49. Greenberg, JH, Reivich M, Alavi A, et al. Metabolic mapping of functional activity in human subjects with the (^{18}F) fluorodeoxyglucose technique. *Science.* 1981;212:678–680.
50. Fox PT, Mintun M, Raichle M, et al. Mapping human visual cortex with positron emission tomography. *Nature.* 1986;323:806–809.
51. Ogawa S, Tank DW, Menon R, et al. Intrinsic signal changes accompanying sensory stimulation: functional brain mapping with magnetic resonance imaging. *Proc Natl Acad Sci USA.* 1992;89:5951–5955.
52. Wu AM, Yazuki PJ, Tsai S-W, et al. MicroPET imaging of tumors in a murine model utilizing a Cu-64 radiolabeled genetically engineered anti-CEA antibody fragment [abstract]. *J Nucl Med.* 1999;40(suppl):80P.
53. Rubins DJ, Melega WP, Cherry SR, Lacan G. Quantitation of striatal dopamine transporter in the rat with [C-11]WIN 25,428 and microPET [abstract]. *J Nucl Med.* 1999;40(suppl):261P.
54. Gambhir SS, Barrio JR, Herschman HR, Phelps ME. Imaging expression: principles and assays. *J Nucl Card.* 1999;6:219–233.
55. Pan D, Gambhir SS, Toyokuni T, et al. Rapid synthesis of a 5′-fluorinated oligodeoxynucleotide: a model antisense probe for use in imaging with positron emission tomography (PET). *Bioorg Med Chem Lett.* 1998;8:1317–1320.
56. Loke SL, Stein CA, Zhang XH, et al. Characterization of oligonucleotide transport into living cells. *Proc Natl Acad Sci USA.* 1989;86:7595–7599.
57. Wu-Pong S, Weiss TL, Hunt AC. Antisense c-myc oligonucleotide cellular uptake and activity. *Antisense Res Dev.* 1994;4:155–163.
58. Crooke ST. Progress in antisense therapeutics. *Hematol Pathol.* 1995;9:59–72.
59. Tavitian B, Terrazzino S, Kuhnast B, et al. In vivo imaging of oligonucleotides with positron emission tomography. *Nature Med.* 1998;4:467–471.
60. Misteli T, Spector D. Applications of the green fluorescent protein in cell biology and biotechnology. *Nat Biotechnol.* 1997;15:961–964.
61. Jacobs WR, Barletta RG, Udani R, et al. Rapid assessment of drug susceptibilities of mycobacterium tuberculosis by means of luciferase reporter phages. *Science.* 1993;260:819–822.
62. Satyamurthy N, Barrio JR, Bida GT, Huang SC, Mazziotta JC, Phelps ME. 3-(2′-[^{19}F]fluoroethyl)spiperone, a potent dopamine antagonist: synthesis, structural analysis and in vivo utilization in humans. *J Appl Rad Isot.* 1990;41: 113–129.
63. Tjuvajev JG, Stockhammer G, Desai R, et al. Imaging the expression of transfected genes in vivo. *Cancer Res.* 1995;55:6126–6132.
64. Tjuvajev JG, Finn R, Watanabe K, et al. Noninvasive imaging of herpes virus thymidine kinase gene transfer and expression: a potential method for monitoring clinical gene therapy. *Cancer Res.* 1996;56:4087–4095.
65. Tjuvajev JG, Avril N, Safer M, et al. Quantitative PET imaging of HSV1-TK gene expression with [1–124]FIAU [abstract]. *J Nucl Med.* 1997;38(suppl):239P.
66. Barrio JR, Namavari M, Phelps ME, et al. Regioselective fluorination of substituted guanines with dilute F2: a facile entry of 8-fluoroguanine derivatives. *J Organic Chem.* 1996;61:6084–6085.
67. Gambhir SS, Barrio JR, Wu L, et al. Imaging of adenoviral directed herpes simplex virus type 1 thymidine kinase reporter gene expression in mice with radiolabeled ganciclovir. *J Nucl Med.* 1998;39:2003–2011.
68. Gambhir SS, Barrio JR, Phelps ME, et al. Imaging adenoviral-directed reporter gene expression in living animals with positron emission tomography. *Proc Natl Acad Sci USA.* 1999;96:2333–2338.
69. Namavari N, Barrio JR, Gambhir SS, et al. Synthesis of 8-[^{18}F]fluoroguanine derivatives: in vivo probes for imaging gene expression with PET. *Nucl Med Biol.* 2000: in press.
70. Gambhir SS, Barrio JR, Herschman HR, Phelps ME. Assays for non-invasive imaging of reporter gene expression. *Nucl Med Biol.* 1999;26:481–490.
71. Gambhir SS, Barrio JR, Iyer M, et al. In vivo validation of PET reporter gene/reporter probe assay for herpes simplex virus type 1 thymidine kinase with 8-[F-18]-fluoropenciclovir [abstract]. *J Nucl Med.* 1999;40(suppl):25P–26P.
72. Alauddin MM, Conti PS. Synthesis and preliminary evaluation of 9-(4-[18F]-fluoro-3-hydroxymethylbutyl)guanine ([^{18}F]FHBG): a new potential imaging agent for viral infection and gene therapy using PET. *Nucl Med Biol.* 1998;25: 175–180.
73. MacLaren DC, Gambhir SS, Satyamurthy N, et al. Repetitive non-invasive imaging of the dopamine D2 receptor as a reporter gene in living animals. *Gene Ther.* 1999;6:785–791.
74. Gordon EM, Barrett RW, Dower WJ, et al. Applications of combinatorial technologies to drug discovery: part 2. Combinatorial organic synthesis, library screening strategies, and future directions. *J Med Chem.* 1994;10:1385–1401.
75. Satyamurthy N, Barrio JR, Phelps ME. Electronic generators for production of positron-emitter labeled radiopharmaceuticals: where would PET be without them? *Clin Positron Imaging.* 1999;2:233–254.
76. Shao Y, Cherry SR, Farahani K, et al. Development of a PET detector system compatible with MRI/NMR systems. *IEEE Trans Nucl Sci.* 1997;44:1167–1171.
77. Beyer T, Townsend DT, Brun T, et al. A combined PET/CT scanner for clinical oncology. *J Nucl Med.* 2000: in press.
78. Patton JA, Delbeke D, Sandler MP. Image fusion using integrated dual-head coincidence camera with x-ray tube based attenuation maps. *J Nucl Med.* 2000: in press.